American Journal of Engineering Research (AJER)
e-ISSN : 2320-0847 p-ISSN : 2320-0936
Volume-02, Issue-10, pp-441-450
www.ajer.org
Research Paper Open Access

11. $^{208}_{82}$Pb, $^{232}_{90}$Th, $^{256}_{100}$Fm nucleus internal structure and Parameter calculation

11. 1 "Assembly" the principle of atomic nuclei

Pass in front of the internal structure of the nucleus, chapter 7 ~ 10 nuclear force, magnetic forming principle and parameters of calculation, we not only have "assembly" the basis of atomic nuclei, and predictable "assembly" nucleus must abide by the principle of a couple of items. At the same time also will to book model, theory of thorough and the strict proof of simulation.

11.1.1 Nuclear in nucleus, with net charge density distribution Principle, etc

According to the experimental determination results, combined with map 7.1 ~ 7.3 nucleus internal structure model, nuclear power load distribution characteristics. We will nuclear, various high, low-energy particle spiral loop net with $\pi^{\pm}$ "assembly", such as violation of density and tend to be spherical. Lining and internal each particle spiral rings, all shall be according to (9.12) is the result of saturated layer and outer layer and edge can be in a state of unsaturated. That are nucleus boundary there natural "dispersion" layer. Nuclear force action radius including low-energy particles spiral ring outside edge, slightly greater than the net with π_g^+ violation of high-energy particles spiral ring distribution radius. Outside the nucleus edge due to the low particles spiral ring net with π_d^- forces, and conditions within the nucleus edge π_g^+ mesons are weaken the effect of electric field, on the whole reflects the nucleus wrapped in a layer of "neutron skin". These characteristics are shown in figure 7.1 and figure 7.2 are clearly reflected.

11.1.2 Total energy conservation principle

Nucleus total energy is high, low-energy particle spiral ring, all the original $\pi^{\pm}$ muon total energy $\overline{m}_{di}$, $\overline{m}_{gi}$, and the high and low particles spiral rings, each net with $\pi^{\pm}$ muon between spin direction, electric and magnetic field of the interaction of the sum of total energy. Total energy of atoms of each element of the determination of the laboratory, should deduct outside the nucleus of all electronic rest mass $Z_i m_{eo}$, plus all of the electronic ionization energy, (book electronic ionization energy at all). Because all electronic total ionization energy is much smaller than the total energy of the nucleus, so, this book in does not affect the nucleus total energy calculation precision premise, outside the nucleus all electronic total ionization energy estimation values, (see chapter 20 atomic physics).

When protons and neutrons are even nucleus, by (9.8), (9.13), high, low particles spiral ring all $\pi^{\pm}$ in violation of the original total energy is: $\sum m_{\pi} = 5A_i\overline{m}_{d1} + \sum \Delta\overline{m}_{ni}$ (A_i is the sum of the number of protons and neutrons).

Nucleus of different even protons, neutrons, $\pi^{\pm}$ violation of the original total energy calculation should be two steps. Refer to section 7.2 the nuclear magnetic forming principle, the calculation first $5(A_i - 2)\overline{m}_{d1}$ or $5(A_i - 3)\overline{m}_{d1}$ the nucleus of the original total energy; Remaining 2 ~ 3 protons, neutrons should according to the experimental value of nuclear magnetic, analysis, simulation computation 2 ~ 3 protons, neutrons "decentralized" $\pi^{\pm}$ mesons, into the high, low-energy particle distribution state of spiral ring; Then on the basis of the listed in table 9.1 $\overline{m}_{di}$, $\overline{m}_{gi}$, data accumulation respectively.

When we according to the principle of article 1 will be all the protons and neutrons "decentralized" into $\pi^{\pm}$ mesons, filling into each layer in nucleus, various high, low-energy particle spiral ring, we can according to the list of equations (8.16), 9.2 or 9.3 to simulate calculation within the nucleus particles spiral ring, net with$\pi^{\pm}$muon spin direction of interaction between electric and magnetic energy. Table 9.2 and table 9.3 in the high and low particles spiral rings $\pi^{\pm}$ violation of electric parameters, refers to each net with $\pi^{\pm}$ muon relative to the nucleus center for a net with unit of electric charge can parameters. In practical calculation, we can as long as potential parameters from big to small, and then in sequence one by one calculation, high in low-energy particle spiral ring net with $\pi^{\pm}$ violation of, and surrounded by the nucleus of the accumulated net charge left for interaction potential can and their own potential; They all algebra and is all the particles in the nucleus of spiral ring net with $\pi^{\pm}$ mesons in the potential of interaction.

Similarly, we can still by the "assembly" out of the nucleus structure model, by (8.15), (8.16) equations, from inside to outside, step by step calculation conditions within the nucleus layers particles spiral ring, net with$\pi^{\pm}$violation in the spin direction of interaction between magnetic energy and accumulative total magnetic field energy.

11.1.3 Stable electric and magnetic field force balance principle

Forming principle, the parameters derived from the nuclear force, demonstration calculation process is not difficult to forecast: stable nucleus, it should be the whole inside the particles spiral ring, general electric and magnetic field force is evenly balanced; The low-energy particles spiral ring rail tangent particles and the whole spiral ring spin track current is the ampere force between the sum of all should be evenly than nuclear power field force in the nuclear spin axial force. If inside a certain position in the nuclear field force the spin axis of the repelling force is greater than the total ampere force of it, it will lead to internal excess $\pi^{\pm}$ muon adjustment, redistribution, or split the decay, until nuclear force equilibrium is stable. So, we can expect that in 1 ~ 2 principle, under the premise of ${}^{206}_{82}$Pb, ${}^{207}_{82}$Pb, ${}^{208}_{82}$Pb, ${}^{209}_{83}$Bifour kinds of natural and artificial radiation is the end of the nuclear, internal nuclear force balance stable state of the simulation results, should be close to the critical instability. We could start the ${}^{208}_{82}$Pb nucleus as validation book the nucleus internal structure, model, the nuclear force balance stable state parameters of the simulation experiment.

11.1.4 Protons, neutrons, □± muon maintain appropriate proportion Principle

Conditions within the nucleus of protons and neutrons must maintain an appropriate ratio, that is their "decentralized" all the high and low of positive and negative $\pi^{\pm}$ mesons in every high, low-energy particle spiral ring, must according to proper proportion of uniform distribution and orderly, make a high or low for each ring particles spiral orbit of $\pi^{\pm}$ violation of excess and $\pi^{\pm}$ between the violation of the electric field force can attract contain each other, which can satisfy various $\pi^{\pm}$ violation within the individual needs of charged particles expansion deformation, and can make the electric field force of each particle spiral ring can maintain the dynamic balance, the whole is in stable condition, the nucleus to ultimate stability.

11.2 $^{208}_{82}$Pb nucleus internal structure and parameter calculation

11.2.1 Nucleus total energy verification calculation

Laboratory determination: $^{208}_{82}$Pb atomic mass is 207.976658u④; It is the element thorium $^{232}_{90}$Th natural radiation is the end of the nucleus. Outside the nucleus of all the electronic total ionization energy $\sum W_{me}$, we take the approximate:

$$\sum W_{me} = K_{\alpha 2} Z_i \qquad (11.1)$$

Which Z_i is nuclear charge and K_{a2} is atomic inner electronic ionization energy. Determined by laboratory to: K_{a2} = 72794 ev ④, the K_{a2} layer represents the average atomic ionization energy of all electronic.

According to (8.19), (9.13) types $\overline{m}_{di}$, $\overline{m}_{gi}$ value in table 9.1, $^{208}_{82}$Pb nucleus total energy is:

$$\sum {}^{208}_{82}PbW_i = 208 \times 5\overline{m}_{d1} + W_e + W_b + \sum \Delta\overline{m}_{ni} \qquad (11.2)$$

By (11.1), set up atomic mass of ${}^{A}_{z}XM$, must be the original mass of the nucleus $\sum {}^{A}_{z}XW_0$ for:

$$\sum {}^{A}_{z}XW_0 = {}^{A}_{z}XM - Z_i m_{e0} + K_{\alpha 2} Z_i e / c^2 \qquad (11.3)$$

The experimental value generation into (11.3), to: $^{208}_{82}$Pb nucleus of the original total energy:

$$\sum {}^{208}_{82}PbW_0 = 3.452895452 \times 10^{-25} Kg$$

The electronic total ionization energy:

$$\sum W_{me} = 5.969108 Mev = 1.064090616 \times 10^{-29} Kg$$

With reference to the principle of figure 7.2 and section 11.1 1, 2, the design of "assembly" $^{208}_{82}$Pb nucleus structure as shown in figure 11.1, it belongs to type B nucleus. Each layer particles spiral rings layer by (9.12) - the number of nuclear calculation results were taken 6, 12, 18, 22, the outermost for unsaturated layer. Layers, various high, low-energy particles spiral ring of protons, neutrons "decentralized" all $\pi^{\pm}$ source, including the net with $\pi^{\pm}$ violation number arrangement principle and distribution status, see section 7.2. We make each layer particles spiral rings with the net high and low $\pi^{\pm}$ muon total the same, in the nuclear field force and the spin direction under the action of ampere force, position can be adjusted, symmetrical distribution, in order to maintain the balance of nuclear power, magnetic force.

Shown from figure 11.1, the ${}^{208}_{82}$Pb conditions within the nucleus net with $\pi^{\pm}$ violation in the moving direction spin interaction between the electric and magnetic energy calculation procedure is as follows:

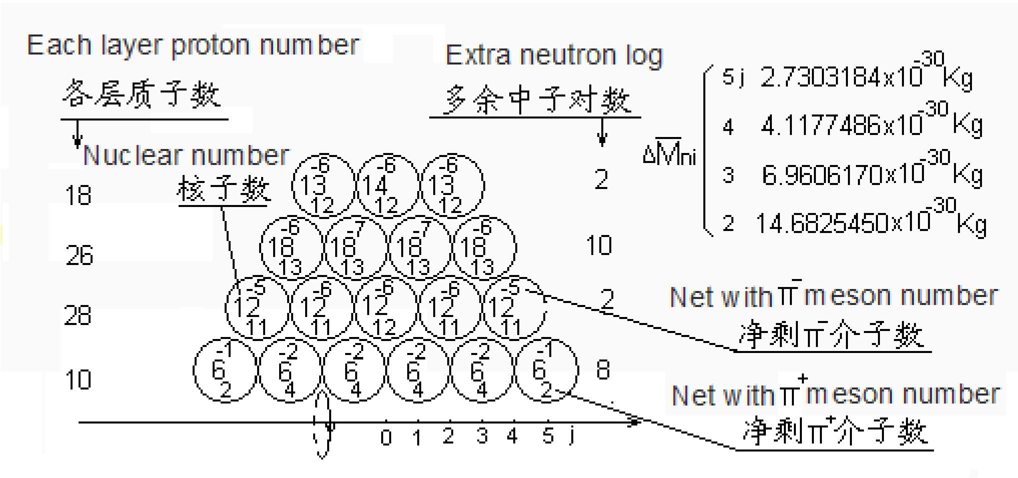

Figure 11.1 ${}^{208}_{82}Pb$ nuclear in nucleus, the net with $\pi^{\pm}$ source distribution

1. By electric potential, as shown in the table 9.3 can parameters, in absolute value from big to small alphabetical order in English first, it represents the net with $\pi^{\pm}$ violation by the nucleus center to the periphery of interaction potential can vary, convenient calculation, the total potential energy.

2. According to the electric potential of a system can sum method, each corresponding layer, the corresponding column of high and low particles spiral rings net with $\pi^{\pm}$ violation number accordingly, written in the letter below arrangement, π_g^{+} number of mesons is positive, π_d^{-} number of violation is negative. To nucleus left and right sides is symmetrical distribution of two pairs of high and low particles spiral rings of the net with$\pi^{\pm}$ violation number should be peace. By (9.13), table 9.1 data: redundant excess energy for the rest of the $\Delta\overline{m}_{ni}$ value is shown in figure 11.1 on the right side.

3. (11.4) - each of the electric potential can be calculated parameters before all the $\pi^{\pm}$ violation of algebra and, on behalf of the particles spiral ring inside relative nucleus surrounded by center of net with nuclear power by number, label in the upper part of the parameters of the electric potential can:

$$\underset{8}{Va}\quad \overset{8}{\underset{-4}{Vb}}\quad \overset{4}{\underset{8}{Vc}}\quad \overset{12}{\underset{-4}{Vd}}\quad \overset{8}{\underset{12}{Ve}}\quad \overset{20}{\underset{-6}{Vf}}\quad \overset{14}{\underset{4}{Vg}}\quad \overset{18}{\underset{22}{Vh}}\quad \overset{40}{\underset{-2}{Vi}}\quad \overset{38}{\underset{-12}{Vj}}$$

$$\overset{26}{\underset{22}{Vk}}\quad \overset{48}{\underset{26}{Vl}}\quad \overset{74}{\underset{-10}{Vm}}\quad \overset{64}{\underset{-14}{Vn}}\quad \overset{50}{\underset{26}{Vo}}\quad \overset{76}{\underset{-12}{Vp}}\quad \overset{64}{\underset{12}{Vq}}\quad \overset{76}{\underset{24}{Vr}}\quad \overset{100}{\underset{-6}{Vs}}\quad \overset{94}{\underset{-12}{Vt}}$$

4. Every high, low-energy particle spiral ring net with $\pi^{\pm}$ both potential can, should be inside relative nucleus center surrounded by the net with total number of nuclear power by the interaction of electric potential energy and its potential. Whole high within the nucleus, low-energy particles spiral loop net with $\pi^{\pm}$ violation of interaction between potential energy, should be each high net, low-energy particle spiral rings with $\pi^{\pm}$ muon interaction potential can be combined. So, directly from the above parameters, we have:

$$W_e = \frac{e}{c^2}\left[\begin{array}{l}\frac{8^2}{2}Va - \left(8\times 4 - \frac{4^2}{2}\right)Vb + \left(4\times 8 + \frac{8^2}{2}\right)Vc - \left(12\times 4 - \frac{4^2}{2}\right)Vd + \\ \cdots\cdots\cdots + \left(76\times 24 + \frac{24^2}{2}\right)Vr - \left(100\times 6 - \frac{6^2}{2}\right)Vs - \left(94\times 12 - \frac{12^2}{2}\right)Vt\end{array}\right] \quad (11.4)$$

The calculation table 9.3 V_{ei} value generations into (11.4), too: W_e = 1.503731485 x 10^{-27} kg

5. By each layer, as shown in the table 9.1, low-energy particle spiral loop quantum fluctuations in N_{adi}, N_{agi} value, respectively into (4.9), speed fluctuation coefficient is obtained β_{gi}, β_{di} value; Along with the generation of (1.6) in type $\overline{m}_{di}, \overline{m}_{gi}$ value, obtained $R_{\theta 0gi}$, $R_{\theta 0di}$ value.

6. Each particle spiral ring of N_{adi}, N_{agi}, β_{gi}, β_{di}, $R_{\theta 0gi}$, $R_{\theta 0di}$ value generation into the type (8.10), respectively, $\overline{R}_{Igi}, \overline{R}_{Idi}$ spiral loop current average radius, are obtained.

7. By figure 11.1 shows, the particles spiral ring layer length coefficient of $K_{bd\,I\,j}$ respectively: K_{bd15} = 12, K_{bd24} = 10, K_{bd33} = 8, K_{bd42} = 6, along with $R_{\theta 0gi}$, $R_{\theta 0di}$, N_{adi},N_{agi} value generation into the equations (8.13), obtained: L_{bgij}, L_{bdij} value.

8. By figure 11.1 shows, the particles spiral ring layer respectively: the number of protons P_1=10, P_2=28, P_3= 26 and P_4=18, along with the above obtained β_{gi}, β_{di}, $\overline{R}_{Igi}$, $\overline{R}_{Idi}$, L_{bgij}, L_{bdij} and N_{adi}, N_{agi} value generation into the equations (8.15), respectively, for magnetic field strength H_{gi}, H_{di} value.

9. The H_{gi}, H_{di}, $\overline{R}_{Igi}$, $\overline{R}_{Idi}$ and L_{bgij}, L_{bdij} value generation into the equations (8.16), respectively, for magnetic energy W_{bgi}, W_{bdi} value.

10. The W_{bgi}, W_{bdi} value accumulation, obtained the total magnetic energy, and conversion for quality, to: $W_b = 1.409748336 \times 10^{-29}\, kg$.

11. By (11.2), too: □ $^{208}_{82}PbW_1$ = 3.452890137 x 10^{-25} kg, compared with the results of the type (11.3), 0.29815 Mev error, is only an outer electrons estimated 5.0% of the total ionization energy, precision has reached the requirement. It can turn to the next topic nuclear force balance test.

12. Figure 11.1 protons and neutrons in nucleus, the distribution of the net with $\pi^{\pm}$ muon state through variety of solutions are the result of the simulation. If default protons, neutrons, and net with $\pi^{\pm}$ source distribution A scheme after 1 ~ 11 calculation program total energy value is not consistent with the experiment, through adjusting the number of protons, neutrons, or particles spiral rings net with $\pi^{\pm}$ both axial distribution, repeated 1 ~ 11 calculation procedures, can change the total energy of the nucleus. That last until agreement with experimental value. (Behind all nuclear source parameters, calculation procedures and adjusting process are the same).

11.2.2 Nuclear force balance test

Shown by table 10.2 B type high within the nucleus, low-energy particles spiral loop net with $\pi^{\pm}$ both between the spin axis nuclear power field force parameters, we can reference potential can the method, step by step, by the calculation of the axial electric field force.

By 1 calculation program of the electric potential can parameters from big to small order, you can clearly see, each pair of high and low particles spiral ring inside relative nucleus center surrounded by the net with nuclear power charge, then itself should be unilateral net with $\pi^{\pm}$ number mesons, symmetrical should be incorporated into the other side of the total number of net with nuclear power charge within the nucleus. So, each pair of high and low particles spiral loop net with $\pi^{\pm}$ violation of A nucleus within the spin axis of the nuclear power field component should be high, low-energy particle spiral ring the axial electric field component. As shown in figure 11.1: layer 2 i= 2, 4 column j = 4 of the particles spiral rings, location code for k, m, by 1 the calculation program of arrangement parameters, we have:

$$F_{e\theta km}=11\times(26+11)F_{e\theta\ k}-5\times(74-5)F_{e\theta m} \qquad (11.5)$$

In the table 10.2 $F_{e\theta k}$, $F_{e\theta m}$ parameters into (11.5), to: $F_{e\theta km}$=570.0909716 (Newton).

Similarly, by (11.5), the parameters in the table 10.2, other particles spiral ring in the nuclear field force of axial component of the results shown in table 11.1.

Within the same layer side by side of low-energy particles spiral ring net with π_d^- both in the spin track tangent of ampere force, from (10.7-1) ~ (10.11) in the derivation process of the type, all is a certainly π_d^- as the basis, when they were N_{e1}, N_{e2} π_d^- violation, the strain (10.11) is:

$$F_{b\theta ij}=N_{e1}N_{e2}F_{kbi} \qquad (11.6)$$

According to the figure 11.1 shows the low-energy particles spiral ring in the net with π_d^- violation number, will each layer in the table 10.3 F_{kbi} parameters, generation into (11.6), respectively, for each track tangent place ampere force shown in table 11.1.

$^{208}_{82}$Pb nucleus kernel force balance test results list (figure 11.1, the unit: Newton) table 11.1

j / N_a	1	2	3	4	5		Nuclear power, the total magnetic force
58 $F_{e\theta}$ $F_{b\theta}$		t. 606.0462530 -534.5717436				↑	689.131672
34 $F_{e\theta}$ $F_{b\theta}$	n. 591.0889169 -936.0859236		p. 1229.43442 -802.3593631			|	617.6571626
16 $F_{e\theta}$ $F_{b\theta}$		j. 991.1342691 -943.7382342		m. 570.0909716 -786.4485285		|	190.5821057
$F_{e\theta}$ 34/13 $F_{b\theta}$ $\Delta F_{\theta b}$	b. 352.235612 -57.06223088		d. 439.5655342 -57.06223088 -137.8927999		i. –13.81634162 -28.53111544 -137.8927999		359.5436277

Note: table 11.1 n column redundant, lower particles on the magnetic force of the spiral ring outside nuclear power field force no set limit; do not participate in the whole nuclear force balance calculation, separated with broad, (the same below).

Adjacent 3 on the high side by side, low-energy particle spiral rings net with $\pi^{\pm}$violation in the spin track movement direction, rail current generated interaction the overall train of ampere force $\triangle F_{\theta bij}$, by (10.17) and K_{fb} parameters, according to the figure 11.1 shows the first layer of particles spiral rings of the net with $\pi^{\pm}$ violation number, we will be the first layer of the calculated value is also listed in table 11.1.

11.2.3 Orbit tangent place ampere force analysis and whole nuclear force balance principle

From table 11.1 that: the entire $^{208}_{82}Pb$ conditions within the nucleus particles spiral ring axial nuclear power field force close to the inside of the ampere force in general; Especially the outer layer $F_{e\theta 42}$ and inner layer $F_{e\theta 22}$, are close to ampere force (the same layer of electric and magnetic field force can accumulate); Overall close to unstable state of the critical limits, and the expected results. At the same time, the first layer of the edge of the particles spiral ring $F_{e\theta 15} << F_{b\theta} + \triangle F_{b\theta}$, even negative, appear to compress the together! From 1 calculation program CLP energy parameters are top of the net with nuclear power charge number see: they are all positive, and that the high and low particles spiral ring in nuclear power, magnetic field force along axial force is not in a state of tension, but in the compressed state within the nucleus.

Further analysis low-energy particles spiral ring rail side by side on the intersec ting ampere force, we found that, it not only in tensile state phase to resist tensile, more in the compression state show the repelling force to resist the effect of compression, but also with the size of the nuclear power field force to adjust! Table 10.3 the calculation of parameters of ampere force is in tension or compression under the two states are of great value. (the characteristics of the nuclear force is also in the field of astronomy neutron stars and black holes internal resistance gravity field of the strong force, see chapter 26)

See figure 10.2 and figure 10.3 and figure 10.4, in the compression state, rail tangent place π_d^- both positive and load in the formation of charged particles is not the current a\`b\` some overlap, but in ab points coincide. Orbit between the tangents of ampere force to showed in figure 11.2. Even though mutual attraction, as long as the largest ampere force is still greater than nuclear power field force in axial compression force, on the whole still can prevent A and B low-energy particles spiral ring in orbit tangent place further compressed cross-border, so disconnect.

Similarly, if the rail tangent electric dipole rotation diameter line a—a\`, b—b\` symmetric intersection as shown in figure 10.3, from chapter 2 elementary particle energy origin of what we already know: elementary particles energy is the wave speed βc, radius of R_a, N_a quantum fluctuations for constituting and electric dipole rotation angle, a rotation radius $K_r \overline{R}_\alpha$, electric dipole log n key parameters comprehensive

decision. So the outside of the electric and magnetic field strength unless to big enough to change its energy, otherwise can't change the key parameters, including, figure 11.2 and figure 10.4 (10.6 1) type of a, Φ value. So, current yuan a—a\`、b—b\` wire under the action of ampere force won't turn around the intersection, can only translation from figure 10.4 tensile state to figure 11.2 state of compression, symmetrical figure 10.3 in the middle position, ampere force general resultant force is zero. By (10.9) ~ (10.11) of integral upper and lower boundaries can be seen, the value of the ampere force in the process of translation will gradually change.

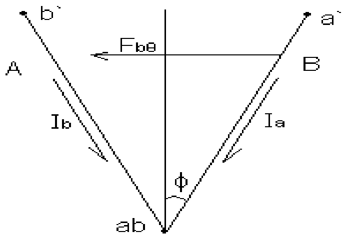

Figure 11.2 I_a and I_b current yuan between ampere force diagram

Thus safely draw the conclusion that each pair of high and low particles spiral ring by nuclear power field force in the spin axis of reality, as long as the rail on the tangent of Ampere force is less than, equal to the maximum, whether tensile force, compression force, or Ampere force will react like spring, and with a—a`, b—b` line of translation, Ampere force will adjust to with nuclear power field force is equal. When nuclear power field repelling force is greater than the left tangent of ampere force, on the tangent of Ampere force reached the maximum. If there is no other force in overcoming nuclear power field force, is where particles spiral rings net with $\pi^{\pm}$ violation will be unstable state.

Economical adjacent particles spiral rings net with $\pi^{\pm}$overall interaction between violation of ampere force, it will be like spring series, the lateral Ampere force accumulate step by step to the inside. Similarly, inside the nuclear field of repelling force is greater than the left tangent of Ampere force; the spare part will accumulate to the outside edge.

Nucleus from figure 11.1 internal layers particles spiral ring stagger Mosaic structure that: as long as the total ampere force is greater than the total nuclear power field, the outside of the inner ring particles spiral foreign the medial layer of particles spiral ring there are space limits to maintain stability. As shown in figure 11.1 in addition to the F_{eBl} and that of high, low-energy particle spiral ring outside, other particles spiral ring embedded structure can be accumulated by the electric and magnetic field force transmission from inner to outer, from outside to inside of the nucleus in general stability of nuclear force balance calculation. From table 11.1 balance accumulated as A result, the nucleus is slightly less than nuclear power of ampere force field force, so the nucleus is not stable, we must to "assemble" $^{208}_{82}$Pb nucleus.

When we adjust figure 11.1 $^{208}_{82}Pb$ within the nuclei of protons, neutrons, the distribution of the net with $\pi^{\pm}$ mesons, can "assembly" out another kind of structure of the $^{208}_{82}Pb$ nucleus, see figure 11.3. According to this section 1 ~ 11 calculation procedure, W_b, W_e, the left figure 11.3 $\sum {}^{208}_{82}Pb$ W_3 value.

Similarly, refer to section nuclear force balance verification calculation method, the results shown in table 11.2.

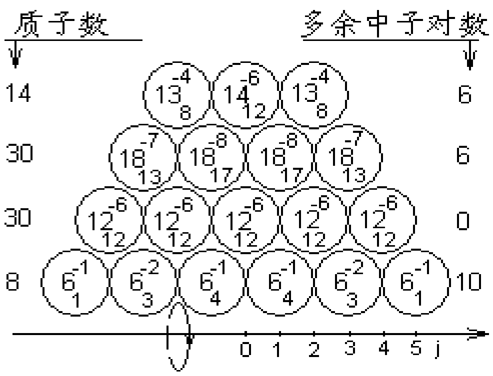

图 11.3 $^{208}_{82}Pb$ 原子核内核子、净剩 $\pi^{\pm}$ 介子分配示意图

Va_{8}	Vb_{-2}^{8}	Vc_{6}^{6}	Vd_{-4}^{12}	Ve_{12}^{8}	Vf_{-6}^{20}
Vg_{2}^{14}	Vh_{24}^{16}	Vi_{-2}^{40}	Vj_{-12}^{38}	Vk_{24}^{26}	Vl_{34}^{50}
Vm_{-12}^{84}	Vn_{-16}^{72}	Vo_{26}^{56}	Vp_{-14}^{82}	Vq_{12}^{68}	Vr_{16}^{80}
Vs_{-6}^{96}	Vt_{-8}^{90}				

$$W_e = 1.549177931\times10^{-27}\,Kg$$
$$W_b = 9.813269321\times10^{-30}\,Kg$$
$$\sum {}^{208}_{82}PbW_3 = 3.452894394\times10^{-25}\,Kg$$

Nucleus $^{208}_{82}Pb$ kernel force balance to verify results (figure 11.3, unit: N) table 11.2

j / N_a	1	2	3	4	5		nuclearElectric and magnetic field force accumulated
58 $F_{e\theta}$ $F_{b\theta}$		t. 410.7162380 -356.3811624				↑	-136.2029571
34 $F_{e\theta}$ $F_{b\theta}$	n. 909.3596443 -1222.642839		p. 1204.566227 -1069.812484			|	-190.5380327
16 $F_{e\theta}$ $F_{b\theta}$		j. 1091.575393 -943.7382342		m. 260.1473009 -943.7382342		|	-325.2917757
$F_{e\theta}$ 34/13 $F_{b\theta}$ $\Delta F_{\theta b}$	b. 520.2435589 -14.26555772 -160.8749332		d. 316.4391041 -28.53111544 -183.8570665		i. –179.5180316 -28.53111544 -30.64284441	|	210.4619988

Obviously, this kind of $^{208}_{82}Pb$ nucleus is stable, is we are looking forward to a solution, compared with the first nuclear model in figure 11.1, key in 1 ~ 2 layer net with $\pi^{\pm}$mesons are different.

11.3 $^{232}_{90}$ Th nucleus internal structure and parameter Calculation

$^{232}_{90}$ Th the nucleus is the natural radiation is thorium is starting, half-life 1.4 x 10^{10}, abundance of 100%.

Laboratory determination $^{232}_{90}$ Th atomic mass is 232.038074 u, inner electronic K_{a2} ionization energy for 89942 ev.

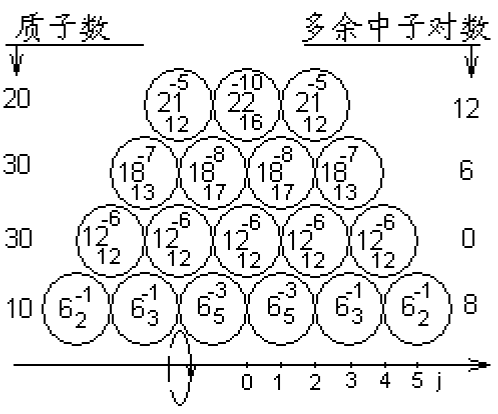

图 11.4 $^{232}_{90}Th$ 原子核内核子、净剩 $\pi^{\pm}$ 介子分配示意图

$$\underset{10}{Va}\quad \overset{10}{\underset{-6}{Vb}}\quad \overset{4}{\underset{6}{Vc}}\quad \overset{10}{\underset{-2}{Vd}}\quad \overset{8}{\underset{12}{Ve}}\quad \overset{20}{\underset{-6}{Vf}}$$

$$\overset{14}{\underset{4}{Vg}}\quad \overset{18}{\underset{24}{Vh}}\quad \overset{42}{\underset{-2}{Vi}}\quad \overset{40}{\underset{-12}{Vj}}\quad \overset{28}{\underset{24}{Vk}}\quad \overset{52}{\underset{34}{Vl}}$$

$$\overset{86}{\underset{-12}{Vm}}\quad \overset{74}{\underset{-16}{Vn}}\quad \overset{58}{\underset{26}{Vo}}\quad \overset{84}{\underset{-14}{Vp}}\quad \overset{70}{\underset{16}{Vq}}\quad \overset{86}{\underset{24}{Vr}}$$

$$\overset{110}{\underset{-10}{Vs}}\quad \overset{100}{\underset{-10}{Vt}}$$

$$W_e = 1.817530386\times10^{-27}\,Kg$$

$$W_b = 1.437800649\times10^{-29}\,Kg$$

$$\sum {}^{232}_{90}ThW_1 = 3.85240599\times10^{-25}\,Kg$$

$^{232}_{90}$ Th nucleus kernel force balance test results list (figure 11.4, unit: N) table 11.3

N_a \ j	1	2	3	4	5	nuclearElectric and magnetic field force accumulated
58 $F_{e\theta}$ $F_{b\theta}$		t. 769.3464573 -742.460755				65.54941594
34 $F_{e\theta}$ $F_{b\theta}$	n. 935.7967653 -1222.642839	p. 1242.139920 -1069.812484				38.66371364
16 $F_{e\theta}$ $F_{b\theta}$		j. 1177.523760 -943.7382342	m. 332.5403448 -943.7382342]			-133.6637224
$F_{e\theta}$ 34/13 $F_{b\theta}$ $\Delta F_{\theta b}$	b. 474.7645661 -128.3900195 -107.2499554	d. 360.3313781 -42.79667316 -153.2142221	i.-30.52020855 -14.26555772 -114.9106665			243.7486412

By (11.3), to: ${}^{232}_{90}$Th nucleus total energy $\sum {}^{232}_{90}ThW_0$ = 3.852409956 x 10^{-25} kg, 10^{-29} kg.

According to figure 11.1 and figure 11.3, the design of ${}^{232}_{90}$Th nucleus internal structure is shown in figure 11.4 and figure 11.5.

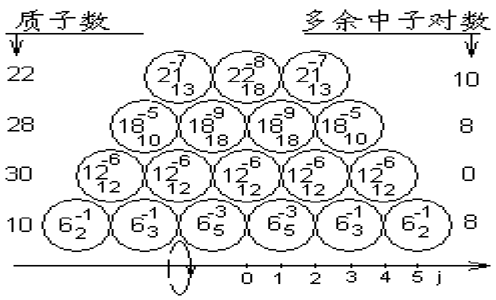

图 11.5 ${}^{232}_{90}Th$ 原子核内核子、净剩 $\pi^{\pm}$ 介子分配示意图

$$Va_{10} \quad Vb^{10}_{-6} \quad Vc^{4}_{6} \quad Vd^{10}_{-2} \quad Ve^{8}_{12} \quad Vf^{20}_{-6}$$

$$Vg^{14}_{4} \quad Vh^{18}_{24} \quad Vi^{42}_{-2} \quad Vj^{40}_{-12} \quad Vk^{28}_{24} \quad Vl^{52}_{36}$$

$$Vm^{88}_{-12} \quad Vn^{76}_{-18} \quad Vo^{58}_{20} \quad Vp^{78}_{-10} \quad Vq^{68}_{18} \quad Vr^{86}_{26}$$

$$Vs^{112}_{-8} \quad Vt^{104}_{-14}$$

$$W_e = 1.812742002 \times 10^{-27} Kg$$

$$W_b = 1.434229785 \times 10^{-29} Kg$$

$$\sum {}^{232}_{90}ThW_2 = 3.852414607 \times 10^{-25} Kg$$

${}^{232}_{90}Th$ Nucleus kernel force balance to verify the results table (figure 11.5, the unit: Newton) table 11.4

N_a \ j	1	2	3	4	5	nuclearElectric and magnetic field force accumulated
58 $F_{e\theta}$ $F_{b\theta}$		t. 708.9523968 -831.5560456				-186.4876078
34 $F_{e\theta}$ $F_{b\theta}$	n. 969.7887665 -1547.407343	p. 985.2165362 -859.6707462				-63.88395896
16 $F_{e\theta}$ $F_{b\theta}$		j. 1177.523760 -943.7382342	m. 276.7743182 -943.7382342			-189.429749
$F_{e\theta}$ 34/13 $F_{b\theta}$ $\Delta F_{\theta b}$	b. 474.7645661 -128.3900195 -107.2499555	d. 360.3313781 -42.79667316 -153.2142222	i.-30.52020855 -14.26555772 -114.9106666			243.7486412

According to section 11.2 of the calculation procedure and method, ${}^{232}_{90}$Th nucleus kernel force balance test results see table 11.3 and table 11.4.

From table 11.3,11.4 and table 11.3，11.4 the result shows: the first kind of nucleus near critical permanent stable state; Second nuclear although of permanent stable nuclei, but 3 ~ 4 layer between particles spiral high-energy π_g^+ mesons in ring is too concentrated, nuclear power will also lead to uneven field force throughout the nucleus are not stable.

11.4 ${}^{256}_{100}$Fm nucleus internal structure and parameter calculation

11.4.1 ${}^{256}_{100}$Fm A type nucleus internal structure and parameter calculation

Laboratory determination ${}^{256}_{100}$Fm atomic mass is 256.091807u, half-life is only 2.63 hours, the inner of electronic K_{a2} ionization energy for 114926 ev. By (11.3), too: $\sum {}^{256}_{100}\text{Fm}W_0 = 4.251801339 \times 10^{-25}$ kg.

For ${}^{256}_{100}$Fm nucleus more nuclear, we first in 7.1 type A nucleus to the model of "assembly" ${}^{256}_{100}$Fm nucleus.

From table 9.1 and table 10.1 types A nucleus calculation of relevant parameters, refer to section 11.2 calculation procedures and nuclear force balance verification calculation method, the result is shown in figure 11.6 and table 11.5.

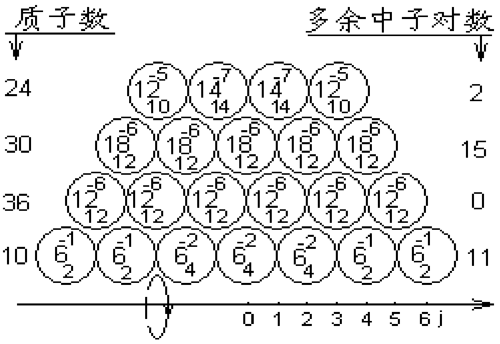

$\underset{4}{Va}$	$\overset{4}{\underset{-2}{Vb}}$	$\overset{2}{\underset{8}{Vc}}$	$\overset{10}{\underset{-4}{Vd}}$	$\overset{6}{\underset{4}{Ve}}$	$\overset{10}{\underset{-2}{Vf}}$
$\overset{8}{\underset{24}{Vg}}$	$\overset{32}{\underset{-12}{Vh}}$	$\overset{20}{\underset{24}{Vi}}$	$\overset{44}{\underset{4}{Vj}}$	$\overset{48}{\underset{-12}{Vk}}$	$\overset{36}{\underset{-2}{Vl}}$
$\overset{34}{\underset{12}{Vm}}$	$\overset{46}{\underset{24}{Vn}}$	$\overset{70}{\underset{-6}{Vo}}$	$\overset{64}{\underset{24}{Vp}}$	$\overset{88}{\underset{-12}{Vq}}$	$\overset{76}{\underset{-12}{Vr}}$
$\overset{64}{\underset{24}{Vs}}$	$\overset{88}{\underset{-12}{Vt}}$	$\overset{76}{\underset{28}{Vu}}$	$\overset{104}{\underset{-14}{Vv}}$	$\overset{90}{\underset{20}{Vw}}$	$\overset{110}{\underset{-10}{Vx}}$

$$W_e = 2.083292346 \times 10^{-27} Kg$$
$$W_b = 1.291733144 \times 10^{-29} Kg$$
$$\sum {}^{256}_{100}FmW_1 = 4.251799043 \times 10^{-25} Kg$$

图 11.6 ${}^{256}_{100}Fm$ 原子核内核子、净剩 $\pi^{\pm}$ 介子分配示意图

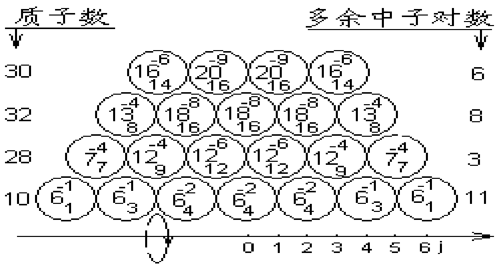

$\underset{4}{Va}$	$\overset{4}{\underset{-2}{Vb}}$	$\overset{2}{\underset{8}{Vc}}$	$\overset{10}{\underset{-4}{Vd}}$	$\overset{6}{\underset{6}{Ve}}$	$\overset{12}{\underset{-2}{Vf}}$
$\overset{10}{\underset{24}{Vg}}$	$\overset{34}{\underset{-12}{Vh}}$	$\overset{22}{\underset{18}{Vi}}$	$\overset{40}{\underset{2}{Vj}}$	$\overset{42}{\underset{-8}{Vk}}$	$\overset{34}{\underset{-2}{Vl}}$
$\overset{32}{\underset{16}{Vm}}$	$\overset{48}{\underset{32}{Vn}}$	$\overset{80}{\underset{-8}{Vo}}$	$\overset{72}{\underset{14}{Vp}}$	$\overset{86}{\underset{-16}{Vq}}$	$\overset{70}{\underset{-8}{Vr}}$
$\overset{62}{\underset{16}{Vs}}$	$\overset{78}{\underset{-8}{Vt}}$	$\overset{70}{\underset{32}{Vu}}$	$\overset{102}{\underset{-18}{Vv}}$	$\overset{84}{\underset{28}{Vw}}$	$\overset{112}{\underset{-12}{Vx}}$

图 11.7 ${}^{256}_{100}Fm$ 原子核内核子、净剩 $\pi^{\pm}$ 介子分配示意图

$$W_e = 2.0724435 25 \times 10^{-27} Kg$$
$$W_b = 1.2310823 09 \times 10^{-29} Kg$$
$$\sum {}^{256}_{100} FmW_2 = 4.251802433 \times 10^{-25} Kg$$

By data can be seen in figure 11.6 and table 11.5:2 ~ 4 layer particles spiral ring inside although magnetic force is greater than the nuclear field force, but on the inside and outside are not embedded space constraints, leading to the bottom and outside layers nuclear power field force far outweigh the magnetic field strength. The nucleus is not stable, also does not exist. We have to redesign "assembly" ${}^{256}_{100}$Fm nucleus. As shown in the figure 11.7 and figure 11.8. Nuclear force balance test results see table 11.6 and table 11.7.

${}^{256}_{100}$Fm nucleus kernel force balance to verify results (figure 11.6, unit: N) table 11.5

j / N_a	1	2	3	4	5	6		nuclearElectric and magnetic field force accumulated
58 $F_{e\theta}$	v. 373.6420907		x. 720.8090694				↑	3276.131632
$F_{b\theta}$	-727.6115399		-519.7225285				|	
34 $F_{e\theta}$		q. 640.1304363		t. 1331.794967			|	3075.045092
$F_{b\theta}$		-687.7365970		-687.7365970			|	
16 $F_{e\theta}$	h. 480.0435425		k. 1054.873673		r. 2378.302662		|	2430.986722
$F_{b\theta}$	-943.7382342		-943.7382342		-943.7382342		|	
$F_{e\theta}$		d. 712.7489433		f. 129.9625756		l. 418.2198398	|	885.286855
34/13 $F_{b\theta}$		-57.06223088		-28.53111544		-14.26555772	|	
$\Delta F_{\theta b}$		-137.8927999		-68.94639993		-68.94639993	|	

By figure 11.6 and figure 11.7 and figure 11.8 and table 11.5 and table 11.6 and table 11.7 the internal structure, nuclear force balance verification calculation parameters is visible, we design three kinds of the nucleus of the difference is very big, $\pi^{\pm}$muon combination scheme, simulation calculation of type A ${}^{256}_{100}$Fm nucleus, the common features are: nucleus layers inside and the outside edge particles spiral ring in the nuclear field force are far outweigh the magnetic force, obviously, the three type A nucleus is very unstable, also won't exist. Further behind on quality of medium to light nuclei of the nuclear force balance test simulation analysis also showed that the number of nuclear power by $Z_i \geq 6$ all the nucleus, type A nucleus are unreliable, can only is type B nucleus. ${}^{256}_{100}$Fm nucleus kernel force balance to verify the results

(Figure 11.7, unit: N) table 11.6

j / N_a	1	2	3	4	5	6		nuclearElectric and magnetic field force accumulated
58 $F_{e\theta}$	v. 356.0835222		x. 1083.090634				↑	2465.520852
$F_{b\theta}$	-1202.786423		-801.8576154				|	
34 $F_{e\theta}$		q.1116.491063		t. 831.9768966			|	2184.287834
$F_{b\theta}$		-1222.642839		-611.3214195			|	

16 $F_{e\theta}$ $F_{b\theta}$	h. 543.0960990 -943.7382324		k. 922.5650244 -629.1588228	r. 1404.572717 -419.4392152	|	1963.632357
$F_{e\theta}$ 34/13 $F_{b\theta}$ $\Delta F_{\theta b}$		d.712.7489433 -57.06223088 -45.96426662	f. 268.7410103 -28.53111544 -191.5177776	l. 79.24720327 -14.26555772 -38.30355552	|	685.0926531

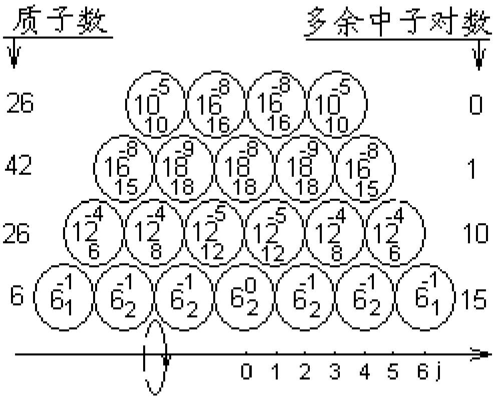

图 11.8 $^{256}_{100}Fm$ 原子核内核子、净剩 $\pi^{\pm}$

介子分配示意图

$$\underset{2}{Va}\quad \overset{2}{\underset{0}{Vb}}\quad \overset{2}{\underset{4}{Vc}}\quad \overset{6}{\underset{-2}{Vd}}\quad \overset{4}{\underset{4}{Ve}}\quad \overset{8}{\underset{-2}{Vf}}$$

$$\overset{6}{\underset{24}{Vg}}\quad \overset{30}{\underset{-10}{Vh}}\quad \overset{20}{\underset{16}{Vi}}\quad \overset{36}{\underset{2}{Vj}}\quad \overset{38}{\underset{-8}{Vk}}\quad \overset{30}{\underset{-2}{Vl}}$$

$$\overset{28}{\underset{18}{Vm}}\quad \overset{46}{\underset{36}{Vn}}\quad \overset{82}{\underset{-8}{Vo}}\quad \overset{74}{\underset{12}{Vp}}\quad \overset{86}{\underset{-18}{Vq}}\quad \overset{68}{\underset{-8}{Vr}}$$

$$\overset{60}{\underset{30}{Vs}}\quad \overset{90}{\underset{-16}{Vt}}\quad \overset{74}{\underset{32}{Vu}}\quad \overset{106}{\underset{-16}{Vv}}\quad \overset{90}{\underset{20}{Vw}}\quad \overset{110}{\underset{-10}{Vx}}$$

$$W_e = 2.049571000 \times 10^{-27}\, Kg$$

$$W_b = 5.584920854 \times 10^{-30}\, Kg$$

$$\sum {}^{256}_{100}FmW_3 = 4.251799918 \times 10^{-25}\, Kg$$

$^{256}_{100}$ Fm nucleus kernel force balance to verify the results (figure 11.8, unit: N) table 11.7

j / N_a	1	2	3	4	5	6		nuclearElectric and magnetic field force accumulated
58 $F_{e\theta}$ $F_{b\theta}$	v. 423.420591 −950.3497664		x. 720.8090694 −593.968604				↑	1414.655202
34 $F_{e\theta}$ $F_{b\theta}$		q.1271.796258 -1375.473194	t.1528.592936 -1375.473194				|	1287.814736
16 $F_{e\theta}$ $F_{b\theta}$	h. 481.1898312 −655.3737738		k. 670.5780981 −524.299019	r. 1111.131136 −419.4392152			|	1134.694994
$F_{e\theta}$ 34/13 $F_{b\theta}$ $\Delta F_{\theta b}$		d.246.3420037 -22.98213332	f. 94.52093682 -14.26555772 -45.96426665	l. 76.32070266 -14.26555772 -22.98213332			|	296.7239945

11.4.2 $^{256}_{100}$Fm B type nucleus internal structure and parameter Calculation

When we use type B nuclei model to "assemble" $^{256}_{100}$Fm nucleus, see figure 11.9 and figure 11.10, the nuclear force balance test simulation results shown in table 11.8 and table 11.9.

$^{256}_{100}$ Fm nucleus kernel force balance to verify the results (figure 11.9, unit: N) table 11.8

j / N_a	1	2	3	4	5	nuclearElectric and magnetic field force accumulated

88 $F_{e\theta}$ $F_{b\theta}$	v. 63.14830698 -48.38782324			↑	290.5680627
58 $F_{e\theta}$ $F_{b\theta}$		t. 954.9819745 -950.3497664		|	275.8075790
34 $F_{e\theta}$ $F_{b\theta}$	n. 879.4710447 -1547.407343	p. 1583.763385 -1203.539045		|	271.1753709
16 $F_{e\theta}$ $F_{b\theta}$		j. 1177.523760 -943.7382342	m. 332.5403448 -943.7382342	|	-109.0489691
$F_{e\theta}$ 34/13 $F_{b\theta}$ $\Delta F_{\theta b}$	b. 352.2356112 -57.06223088 -91.92853324	d. 238.3761117 -57.06223088 -30.64284441	i. 96.19284851 -28.53111544 -153.2142221	|	268.3633945

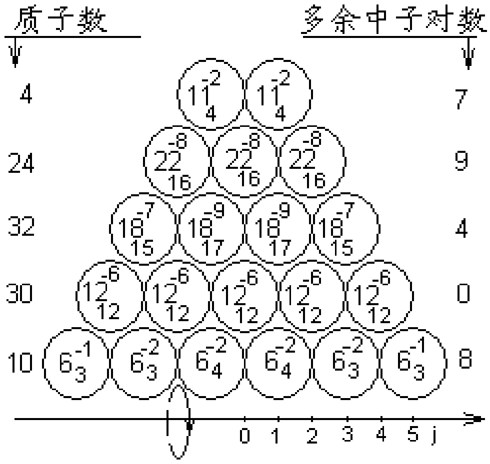

图 11.9 ${}^{256}_{100}Fm$ 原子核内核子、净剩 $\pi^{\pm}$ 介子分配示意图

Va_{8} Vb^{8}_{-4} Vc^{4}_{6} Vd^{10}_{-4} Ve^{6}_{12} Vf^{18}_{-6}

Vg^{12}_{6} Vh^{18}_{24} Vi^{42}_{-2} Vj^{40}_{-12} Vk^{28}_{24} Vl^{52}_{34}

Vm^{86}_{-12} Vn^{74}_{-18} Vo^{56}_{30} Vp^{86}_{-14} Vq^{72}_{16} Vr^{88}_{32}

Vs^{120}_{-8} Vt^{112}_{-16} Vu^{96}_{8} Vv^{104}_{-4}

$$W_e = 2.110556341 \times 10^{-27}\ Kg$$

$$W_b = 1.446182535 \times 10^{-29}\ Kg$$

$$\sum {}^{256}_{100}FmW_4 = 4.251800825 \times 10^{-25}\ Kg$$

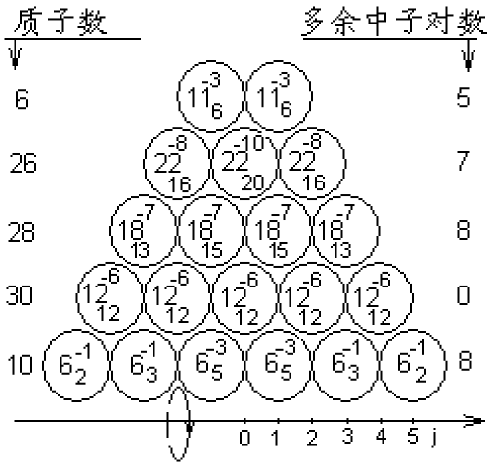

图 11.8 ${}^{256}_{100}Fm$ 原子核内核子、净剩 $\pi^{\pm}$ 介子分配示意图

Va_{10} Vb^{10}_{-6} Vc^{4}_{6} Vd^{10}_{-2} Ve^{8}_{12} Vf^{20}_{-6}

Vg^{14}_{4} Vh^{18}_{24} Vi^{42}_{-2} Vj^{40}_{-12} Vk^{28}_{24} Vl^{52}_{30}

Vm^{82}_{-12} Vn^{70}_{-14} Vo^{56}_{26} Vp^{82}_{-14} Vq^{68}_{20} Vr^{88}_{32}

Vs^{120}_{-10} Vt^{110}_{-16} Vu^{94}_{12} Vv^{106}_{-6}

$$W_e = 2.096575583 \times 10^{-27}\ Kg$$

$$W_b = 1.437941511 \times 10^{-29}\ Kg$$

$$\sum {}^{256}_{100}FmW_5 = 4.251801656 \times 10^{-25}\ Kg$$

${}^{256}_{100}$Fm nucleus kernel force balance to verify results (figure 11.10, unit: N) table 11.9

j / N_a	1	2	3	4	5		nuclearElectric and magnetic field force accumulated
88 $F_{e\theta}$ $F_{b\theta}$	v. 93.99510946 -108.8726023					↑	11.8867131
58 $F_{e\theta}$ $F_{b\theta}$		t. 968.3527797 -1187.937208				|	26.76420594
34 $F_{e\theta}$ $F_{b\theta}$	n. 813.0135219 -936.0859236	p. 1204.566227 -936.0859236				|	246.3486342
16 $F_{e\theta}$ $F_{b\theta}$		j. 1177.523760 -943.7382342	m. 444.0723980 -943.7382342			|	-22.13166916
$F_{e\theta}$ 34/13 $F_{b\theta}$ $\Delta F_{\theta b}$	b. 474.7645661 -128.3900195 -107.2499554	d. 360.3313781 -42.79667316 -153.2142221	i. -30.52020855 -14.26555772 -114.9106665				243.7486412

By figure 11.9 and figure 11.10 and table 11.8 and table 11.9 the results can be seen, with both the internal structure of the nucleus ${}^{256}_{100}$Fm, accumulative total nuclear power field force is only slightly greater than the magnetic field strength. Such as column of table 11.9 v, t, although ampere force is greater than the nuclear field, as a result of p particles in the column spiral ring no set limit, although that is unstable nuclei, but there can temporarily.

From this chapter three atoms of ${}^{208}_{82}$Pb, ${}^{232}_{90}$Th, ${}^{256}_{100}$Fm the internal structure of nuclide in the design, simulation results can be seen that: in the nuclear in nucleus, net with $\pi^{\pm}$muon uniform distribution, under the premise of to "assemble" out of accord with a stable nuclei of the total energy of only a few solutions, which can only individual with internal nuclear force balance condition, but this individual (not only) example also shows that exist with nuclear power.

12 ${}^{168}_{70}$Yb, ${}^{124}_{54}$Xe, ${}^{54}_{26}$Fe, ${}^{40}_{20}$Ca, ${}^{16}_{8}$O maintenance Nuclei and stable isotope internal structure And parameter Calculation

12.1 ${}^{168}_{70}$Yb nucleus and stable isotope internal structure And parameter calculation

12.1.1 ${}^{168}_{70}$Yb nucleus and stable isotopes experiment, parameters calculated value

The scientific community has been found that thousands of nuclide, of which only hundreds of stable isotopes. This chapter will purposefully selected the above five kinds of nuclei and isotope, internal structure design, analysis and parameter calculation, so as to fully verify the theoretical model.

$^{168}_{70}$Yb nucleus and stable isotopes energy parameters experiment results table 12.1

Nuclide	The determination of total energy atomic u	Abundance %	Nucleus total energy calculated value x 10^{-25} kg	Net with $\pi^{\pm}$ source electromagnetic field total energy x 10^{-27} kg	Magnetic moment U_P Mri son
$^{168}_{70}$Yb	167.933925	0.14	2.788036725	1.228920997	
$^{170}_{70}$Yb	169.934792	3.0	2.821261926	1.246979758	
$^{171}_{70}$Yb	170.936354	14.3	2.837893265	1.257883058	0.4919
$^{172}_{70}$Yb	171.936405	21.9	2.854499514	1.266277282	
$^{173}_{70}$Yb	172.938234	16.2	2.871135287	1.277623947	-0.678
$^{174}_{70}$Yb	173.938881	31.8	2.887751433	1.287007853	
$^{176}_{70}$Yb	175.942582	12.7	2.921023694	1.309772585	

$^{168}_{70}$Yb nuclide is total of seven kinds of stable isotopes. In laboratory determination of atoms of each isotope total energy, deduct nucleus all electronic original total energy 70 m_{eo}, plus by (11.1) to estimate the total ionization energy of nuclear electronic 70 x 51326 ev= 6.404786 x10^{-30} kg, obtained $^{168}_{70}$Yb nucleus and stable isotopes energy parameters experiment, the results shown in table 12.1.

Among them, the $\pi^{\pm}$source electromagnetic field temporarily takes no account of $\overline{m}_{di}$, $\overline{m}_{gi}$ and $\overline{m}_{d1}$, $\overline{m}_{g1}$ the energy difference between (the same below).

From table 12.1 that: increases with number of neutrons in the nucleus, nucleus of the particles spiral rings net with $\pi^{\pm}$muon spin direction of the electric and magnetic energy gradually increases, it will be for us in the "assembly", adjusting and simulation nucleus total energy provides the net with $\pi^{\pm}$ source distribution state.

12.1.2 $^{172}_{70}$Yb nucleus internal structure and parameter calculation

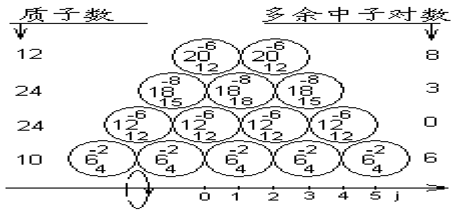

图 12.1 $^{172}_{70}Yb$ 原子核内核子、净剩 $\pi^{\pm}$

介子分配示意图

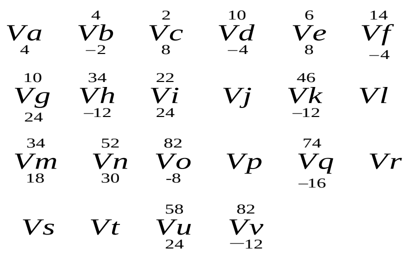

$$W_e = 1.195446297 \times 10^{-27}\, Kg$$

$$W_b = 1.647200661 \times 10^{-29}\, Kg$$

$$\sum {}^{172}_{70}YbW_1 = 2.854494163 \times 10^{-25}\, Kg$$

Refer to section 11.1 ~ 2, all the particles in the nucleus of solenoid ring "assembly", with net high and low $\pi^{\pm}$ source distribution, energy simulation and fitting adjustment process. First to "assemble" ${}^{172}_{70}$Yb with type A nuclear nucleus, see figure 12.1. From table 9.2 type A nuclear potential energy parameters, refer to section (11.4), 11.2 5 ~ 13 calculation procedures, the net can be obtained with $\pi^{\pm}$ muon electric, magnetic energy and nuclear energy. From table 10.1 and table 10.1, (10.17) - calculation data, according to (11.5), (11.6) and (11.7), nuclear force balance test results to shown in table 12.2.

${}^{172}_{70}$Yb nucleus kernel force balance test results list 12.2 (figure 12.1)

j / N_a	1	2	3 6	4	5		nuclearElectric and magnetic field force accumulated
58 $F_{e\theta}$ $F_{b\theta}$	v. 247.5951682 -534.5717436					↑	
34 $F_{e\theta}$ $F_{b\theta}$		q. 1243.455159 -1222.642839				|	967.2598644
16 $F_{e\theta}$ $F_{b\theta}$	h. 543.096099 -943.7382342		k. 1260.146427 -943.7382342			|	946.4475444
$F_{e\theta}$ 34/13 $F_{b\theta}$ $\Delta F_{\theta b}$		d. 712.7489433 -57.06223088	f. 307.2004698 -57.06223088 -275.7855997				630.0393516

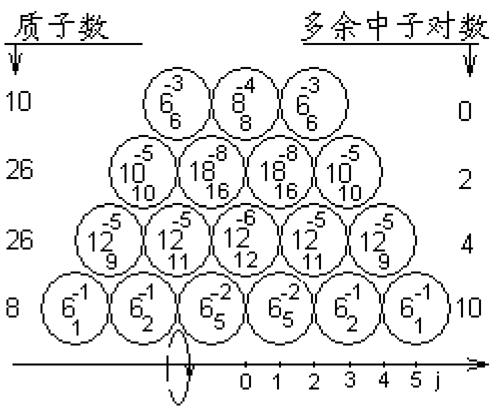

图 12.2 ${}^{172}_{70}Yb$ 原子核内核子、净剩 $\pi^{\pm}$ 介子分配示意图

$Va^{}_{10}$ Vb^{10}_{-4} Vc^{6}_{4} Vd^{10}_{-2} Ve^{8}_{12} Vf^{20}_{-6}

Vg^{14}_{2} Vh^{16}_{22} Vi^{38}_{-2} Vj^{36}_{-10} Vk^{26}_{18} Vl^{44}_{32}

Vm^{76}_{-10} Vn^{66}_{-16} Vo^{50}_{20} Vp^{70}_{-10} Vq^{60}_{8} Vr^{68}_{12}

Vs^{80}_{-4} Vt^{76}_{-6}

$$W_e = 1.184427299 \times 10^{-27}\, Kg$$

$$W_b = 9.366575355 \times 10^{-30}\, Kg$$

$$\sum {}^{172}_{70}YbW_2 = 2.854501194 \times 10^{-25}\, Kg$$

In figure 12.1 $^{172}_{70}$Yb type A nucleus structure model is after many kinds of scheme selection in the simulation of A, all the particles spiral rings net with $\pi^{\pm}$adjusted already tend to limit the distribution of the violation. From can be seen in table 12.2, uneven size of electric and magnetic field distribution in nuclei, especially the bottom, can't set cover the edge spiral ring particles. That is to say: can't stable $^{172}_{70}$Yb "assembly" type A nucleus.

Similarly, when we use type B nuclei model, see figure 12.2:

$^{172}_{70}$Yb nucleus kernel force balance to verify results (figure 12.2, unit: N) table 12.3

j / N_a	1	2	3	4	5		nuclearElectric and magnetic field force accumulated
58 $F_{e\theta}$ $F_{b\theta}$		t. 257.3219278 -178.1905812				↑	-71.2372154
34 $F_{e\theta}$ $F_{b\theta}$	n. 734.3693282 -1222.642839		p. 862.8853063 -764.1517744			|	-150.368562
16 $F_{e\theta}$ $F_{b\theta}$		j. 1033.35848 -786.4485285		m. 32.34284588 -655.3737738		|	-249.1020939
$F_{e\theta}$ 34/13 $F_{b\theta}$ $\Delta F_{\theta b}$	b. 642.7725138 -57.06223088 -306.4284441		d. 237.204948 -28.53111544 -160.8749332		i. -162.8141647 -14.26555744 -22.98213331	|	127.0188825

From table 9.1 and table 9.1 and table 10.2 the calculated data, with reference to the above calculation method, a type B $^{172}_{70}$Yb nucleus internal structure parameters and nuclear force balance test results shown in table 12.3.

12.1.3 $^{170}_{70}$Yb nucleus internal structure and parameter calculation

Similarly, stable isotopes of $^{172}_{70}$Yb nucleus $^{170}_{70}$Yb nucleus, we can in the $^{172}_{70}$Yb nucleus, figure 12.2 model "assembly" on the basis of the protons, neutrons, $\pi^{\pm}$ source distribution adjust state for the internal structure and related parameters.

As shown in the figure 12.3, $^{170}_{70}$Yb nucleus nuclear force balance test results shown in table 12.4.

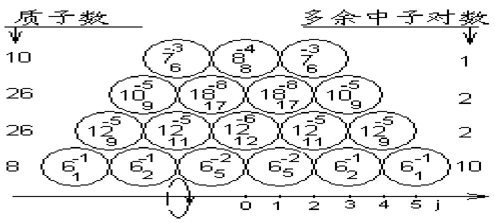

图 12.3 $^{170}_{70}Yb$ 原子核内核子、净剩 $\pi^{\pm}$ 介子分配示意图

$\underset{10}{Va}$ $\overset{10}{\underset{-4}{Vb}}$ $\overset{6}{\underset{4}{Vc}}$ $\overset{10}{\underset{-2}{Vd}}$ $\overset{8}{\underset{12}{Ve}}$ $\overset{20}{\underset{-6}{Vf}}$

$\overset{14}{\underset{2}{Vg}}$ $\overset{16}{\underset{22}{Vh}}$ $\overset{38}{\underset{-2}{Vi}}$ $\overset{36}{\underset{-10}{Vj}}$ $\overset{26}{\underset{18}{Vk}}$ $\overset{44}{\underset{34}{Vl}}$

$\overset{78}{\underset{-10}{Vm}}$ $\overset{68}{\underset{-16}{Vn}}$ $\overset{52}{\underset{18}{Vo}}$ $\overset{70}{\underset{-10}{Vp}}$ $\overset{60}{\underset{8}{Vq}}$ $\overset{68}{\underset{12}{Vr}}$

$\overset{80}{\underset{-4}{Vs}}$ $\overset{76}{\underset{-6}{Vt}}$

$$W_e = 1.190401554\times 10^{-27}\,Kg$$

$$W_b = 9.366575355\times 10^{-30}\,Kg$$

$$\sum {}^{170}_{70}YbW_1 = 2.82126385\times 10^{-25}\,Kg$$

${}^{170}_{70}$Yb nucleus kernel force balance to verify results (figure 12.3, unit: N) table 12.4

N_a \ j	1	2	3	4	5	nuclearElectric and magnetic field force accumulated	
58 $F_{e\theta}$ $F_{b\theta}$		t. 257.3219278 -178.1905812				↑	-251.3859595
34 $F_{e\theta}$ $F_{b\theta}$	n. 814.2375529 -1222.642839		p. 729.2082511 -764.1517744			|	-330.5173061
16 $F_{e\theta}$ $F_{b\theta}$		j. 1033.35848 -786.4485285		m. -14.12884298 -655.3737738		|	-295.5737828
$F_{e\theta}$ 34/13 $F_{b\theta}$ $\Delta F_{\theta b}$	b. 642.7725138 -57.06223088 -306.4284441		d. 237.204948 -28.53111544 -160.8749332		i. -162.8141647 -14.26555772 -22.98213331		127.0188825

12.1.4 ${}^{173}_{70}$Yb nucleus internal structure and parameter calculation

${}^{173}_{70}$Yb inside protons and neutrons are not even, nuclei are U = 0.678 U_P strength. Because a single nuclear for m_n+2 m_p, according to section 7.2 magnetic moment within the nucleus formation principle, we make the m_n + 2 m_p "decentralized" all the $\pi^{\pm}$ violation, as shown in figure 7.4 a, d, d to plan in each layer, low-energy particle spiral ring rail. By (7.6-4), nuclear magnetic synthesis solution for:

$$\sum U = 5U^{+}_{g1} + U^{-}_{d1} + 2U^{-}_{d2} + U^{-}_{d3} + U^{+}_{d4} \qquad (12.1)$$

Will each to $\pi^{\pm}$ mesons in table 9.1 the original magnetic moment of value generation into (12.1), and converted to MRI son have to: $\sum U = -0.6756U_p$.

From table 9.1 of the $\pi^{\pm}$ muon $\overline{m}_{di}$, $\overline{m}_{gi}$, data quality, m_n + 2 m_p "decentralized" of the $\pi^{\pm}$ violation according to (12.1) of the scheme in the high and low particles spiral ring, the m_n+2m_p total quality, quality will be increased by:$\triangle m=1.213303744\times 10^{-29}$Kg.

So, ${}^{173}_{70}$Yb total energy equation of nucleus $\sum {}^{173}_{70}$ YbW_1 should be expressed as:

$$\sum {}^{173}_{70}YbW_1 = 173\times 5\overline{m}_{d1} + \Delta m + \sum N_i \overline{m}_{ni} + W_b + W_e \qquad (12.2)$$

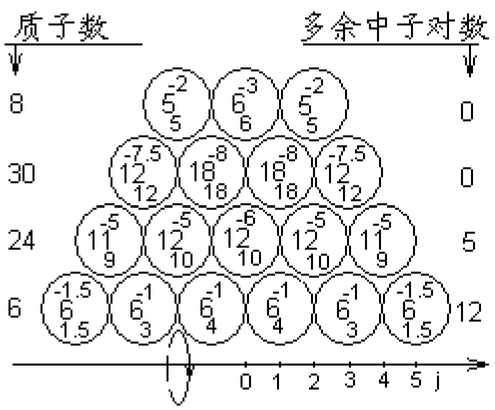

图 12.4 ${}^{173}_{70}Yb$ 原子核内核子、净剩 $\pi^{\pm}$ 介子分配示意图

$\underset{8}{Va}$ $\overset{8}{\underset{-2}{Vb}}$ $\overset{6}{\underset{6}{Vc}}$ $\overset{12}{\underset{-2}{Vd}}$ $\overset{10}{\underset{10}{Ve}}$ $\overset{20}{\underset{-6}{Vf}}$

$\overset{14}{\underset{3}{Vg}}$ $\overset{17}{\underset{20}{Vh}}$ $\overset{37}{\underset{-3}{Vi}}$ $\overset{34}{\underset{-10}{Vj}}$ $\overset{24}{\underset{18}{Vk}}$ $\overset{42}{\underset{36}{Vl}}$

$\overset{78}{\underset{-10}{Vm}}$ $\overset{68}{\underset{-16}{Vn}}$ $\overset{52}{\underset{24}{Vo}}$ $\overset{76}{\underset{-15}{Vp}}$ $\overset{61}{\underset{6}{Vq}}$ $\overset{67}{\underset{10}{Vr}}$

$\overset{77}{\underset{-3}{Vs}}$ $\overset{74}{\underset{-4}{Vt}}$

$$W_e = 1.182004425 \times 10^{-27}\,Kg$$

$$W_b = 1.051690152 \times 10^{-29}\,Kg$$

$$\sum {}^{173}_{70}YbW_1 = 2.871139719 \times 10^{-25}\,Kg$$

According to the above scheme, design of ${}^{173}_{70}Yb$ nucleus to showed in figure 12.4. Convenient for calculating, we will be alone $\pi^{\pm}$ violation "into" two and a half to nuclear power charge number calculation. This does not mean that charged particles can "decentralized", on the contrary, ${}^{173}_{70}Yb$ nucleus of electric quadrupole moment love you just book the correctness of the model and charged particles cannot "disassemble. ${}^{173}_{70}Yb$ Nucleus kernel force balance test results shown in table 12.5.

${}^{173}_{70}Yb$ Nucleus kernel force balance to verify results (figure 12.4, unit: N) table 12.5

j / N_a	1	2	3	4	5		nuclearElectric and magnetic field force accumulated
58 $F_{e\theta}$ $F_{b\theta}$		t. 236.6909889 -89.0952906				↑	-389.2552892
34 $F_{e\theta}$ $F_{b\theta}$	n. 867.6686567 -1222.642839		p. 891.0114236 -1146.227662			|	-536.8509875
16 $F_{e\theta}$ $F_{b\theta}$		j. 920.3767317 -786.4485285		m. -110.2481458 -655.3737738		|	-281.6347491
$F_{e\theta}$ 34/13 $F_{b\theta}$ $\Delta F_{\theta b}$	b. 520.2435589 -14.26555772 - 107.2499554		d. 473.2387324 -14.26555772 -210.6695553		i. –218.119028 -21.39833658 -57.45533327		350.0589672

12.1.5 ${}^{168}_{70}$Yb nucleus internal structure and parameter calculation

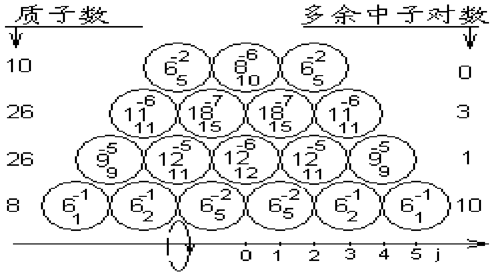

图 12.5 ${}^{168}_{70}Yb$ 原子核内核子、净剩 $\pi^{\pm}$

介子分配示意图

Va_{10} Vb^{10}_{-4} Vc^{6}_{4} Vd^{10}_{-2} Ve^{8}_{12} Vf^{20}_{-6}

Vg^{14}_{2} Vh^{16}_{22} Vi^{38}_{-2} Vj^{36}_{-10} Vk^{26}_{18} Vl^{44}_{30}

Vm^{74}_{-10} Vn^{64}_{-14} Vo^{50}_{22} Vp^{72}_{-12} Vq^{60}_{10} Vr^{70}_{10}

Vs^{80}_{-6} Vt^{74}_{-4}

$$W_e = 1.18362812\times10^{-27}\,Kg$$

$$W_b = 9.3665753\!5\!5\times10^{-30}\,Kg$$

$$\sum {}^{168}_{70}YbW_1 = 2.788033106\times10^{-25}\,Kg$$

${}^{168}_{70}Yb$ Nucleus kernel force balance to verify results (figure 12.5, unit: N) table 12.6

j / N_a	1	2	3	4	5		nuclearElectric and magnetic field force accumulated
58 $F_{e\theta}$ $F_{b\theta}$		t. 251.5671654 -178.1905812				↑	-37.68937437
34 $F_{e\theta}$ $F_{b\theta}$	n. 705.4066273 -936.0859236		p. 893.9238096 -802.3593631			|	-111.0659586
16 $F_{e\theta}$ $F_{b\theta}$		j. 1033.35848 -786.4485285		m. 78.81453473 -655.3737738		|	-202.6304051
$F_{e\theta}$ 34/13 $F_{b\theta}$ $\Delta F_{\theta b}$	b. 642.7725138 -57.06223088 -306.4284441		d. 237.204948 -28.53111544 -160.8749332		i.–162.8141647 -14.26555772 -22.98213331	|	127.0188825

Similarly, refer to section 12.1.2 ~ 12.1.3, ${}^{168}_{70}$Yb nucleus internal structure and the nuclear force balance verification calculation is shown in figure 12.5 and table 12.6.

12.1.6 Y ${}^{174}_{70}$ b nucleus internal structure and parameter calculation

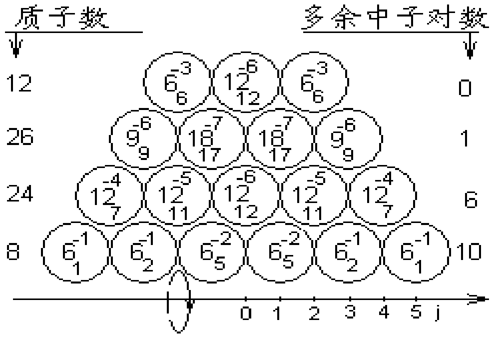

介子分配示意图

Va_{10} Vb^{10}_{-4} Vc^{6}_{4} Vd^{10}_{-2} Ve^{8}_{12} Vf^{20}_{-6}

Vg^{14}_{2} Vh^{16}_{22} Vi^{38}_{-2} Vj^{36}_{-10} Vk^{26}_{14} Vl^{40}_{34}

Vm^{74}_{-8} Vn^{66}_{-14} Vo^{52}_{18} Vp^{70}_{-12} Vq^{58}_{12} Vr^{70}_{12}

Vs^{82}_{-6} Vt^{76}_{-6}

图 12.6 ${}^{174}_{70}Yb$ 原子核内核子、净剩 $\pi^{\pm}$

$$W_e = 1.182568429 \times 10^{-27} Kg$$
$$W_b = 9.223978353 \times 10^{-30} Kg$$
$$\sum {}^{174}_{70}YbW_1 = 2.887749837 \times 10^{-25} Kg$$

${}^{174}_{70}Yb$ Nucleus kernel force balance to verify results (figure 12.6, unit: N) table 12.7

j / N_a	1	2	3	4	5		nuclearElectric and magnetic field force accumulated
58 $F_{e\theta}$ $F_{b\theta}$		t. 269.2228690 -267.2858718				↑	-418.1139802
34 $F_{e\theta}$ $F_{b\theta}$	n. 795.9492798 -936.0859236	p. 600.3548052 -802.3593631				|	-420.0509774
16 $F_{e\theta}$ $F_{b\theta}$		j. 1033.35848 -786.448285	m. -67.67623443 -524.299019			|	-218.0464195
$F_{e\theta}$ 34/13 $F_{b\theta}$ $\Delta F_{\theta b}$	b. 642.7725138 -57.06223088 -306.4284441	d. 237.204948 -28.53111544 -160.8749332	i.–162.8141647 -14.26555772 -22.98213331				127.0188825

Similarly, refer to section 12.1.2 ~ 12.1.3, 12.1.5, ${}^{174}_{70}$Yb nucleus internal structure and the nuclear force balance verification calculation is shown in figure 12.6 and table 12.7.

12.1.7 ${}^{176}_{70}$Yb nucleus internal structure and parameter calculation

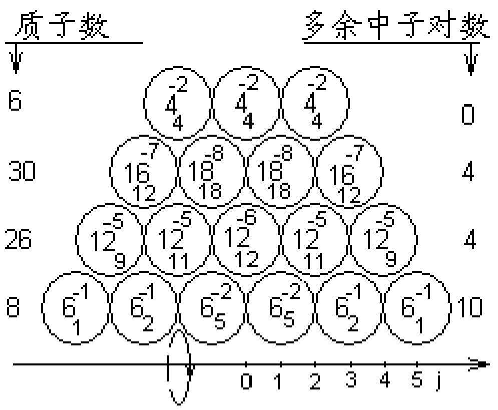

图 12.7 ${}^{176}_{70}Yb$ 原子核内核子、净剩 $\pi^{\pm}$ 介子分配示意图

Va_{10} Vb^{10}_{-4} Vc^{6}_{4} Vd^{10}_{-2} Ve^{8}_{12} Vf^{20}_{-6}

Vg^{14}_{2} Vh^{16}_{22} Vi^{38}_{-2} Vj^{36}_{-10} Vk^{26}_{18} Vl^{44}_{36}

Vm^{80}_{-10} Vn^{70}_{-16} Vo^{54}_{24} Vp^{78}_{-14} Vq^{64}_{4} Vr^{68}_{8}

Vs^{76}_{-2} Vt^{74}_{-4}

$$W_e = 1.214035693 \times 10^{-27} Kg$$
$$W_b = 9.43993031 \times 10^{-30} Kg$$
$$\sum {}^{176}_{70}YbW_1 = 2.921026450 \times 10^{-25} Kg$$

${}^{176}_{70}Yb$ Nucleus kernel force balance to verify results (figure 12.7, unit: N) table 12.8

j / N_a	1	2	3	4	5	nuclearElectric and magnetic field force accumulated	
58 $F_{e\theta}$ $F_{b\theta}$		t. 165.2853417 -59.3968604				↑	-315.4699263
34 $F_{e\theta}$ $F_{b\theta}$	n. 896.5909453 -1222.642839		p. 990.4995480 -1069.812484			|	-421.3584076
16 $F_{e\theta}$ $F_{b\theta}$		j. 1033.35848 -786.4485285		m. -60.60053183 -655.3737738		|	-342.0454716
$F_{e\theta}$ 34/13 $F_{b\theta}$ $\Delta F_{\theta b}$	b. 642.7725138 -57.06223088 -306.4284441		d. 237.204948 -28.53111544 -160.8749332		i. -162.8141647 -14.26555772 -22.98213331		127.0188825

Similarly, referring to the 12.1.5 ~ 12.1.6, internal structure and the ${}^{176}_{70}Yb$ nucleus nuclear force balance verification calculation is shown in figure 12.7 and table 12.8.

12.2 ${}^{130}_{54}$Xe nucleus and stable isotope internal structure and parameter calculation

12.2.1 ${}^{130}_{54}$Xe nucleus and stable isotopes of the calculated value

${}^{130}_{54}$Xe nucleus and stable isotopes parameter experiment, the results table table 12.9

Nuclide	The determination of total energy atomic u	Abundance %	Nucleus total energy calculated value $\times 10^{-25}$Kg	Net with $\pi^{\pm}$ source electromagnetic field total energy $\times 10^{-28}$Kg	Magnetic moment U_P
${}^{124}_{54}$Xe	123.90612	0.096	2.057047409	8.281386454	
	125.904279	0.09	2.090227643	8.417006639	
${}^{126}_{54}$Xe	127.9035323	1.92	2.123426047	8.570798115	
	128.904784	26.44	2.140052234	8.674678462	-0.7768
${}^{128}_{54}$Xe	129.9035108	4.08	2.156636494	8.736631829	
	130.9050847	21.18	2.173268032	8.845862436	0.69066
${}^{129}_{54}$Xe	131.9041568	26.89	2.189858025	8.913549648	
	133.905398	10.44	2.22308944	9.100351003	
${}^{130}_{54}$Xe	135.907222	8.9	2.256330532	9.296829987	
${}^{131}_{54}$Xe					
${}^{132}_{54}$Xe					

$^{134}_{54}$Xe $^{136}_{54}$Xe					

$^{130}_{54}$Xe isotopes and stable isotopes of nine, with reference to the section on $^{168}_{70}$Yb nucleus and table 12.1 the parameters of the calculation method of $^{130}_{54}$Xe nucleus and stable isotopes parameter experimental data, the results shown in table 12.9. Of atoms inside the K_{a2} layer of electronic ionization energy K_{a2} = 29485 ev, generation of (11.1) in type, too: $\sum W_{me}=2.838337718\times10^{-30}Kg$.

12.2.2 $^{130}_{54}$Xe nucleus internal structure and parameter calculation

Refer to section 12.1 $^{172}_{70}$Yb nucleus internal structure and parameter calculation method, the nuclear force balance verification calculation process, we are still in 7.1 type A nucleus model of the first "assembly" $^{130}_{54}$Xe nucleus, see figure 12.8. $^{130}_{54}$Xe nuclear force balance test results shown in table 12.10.

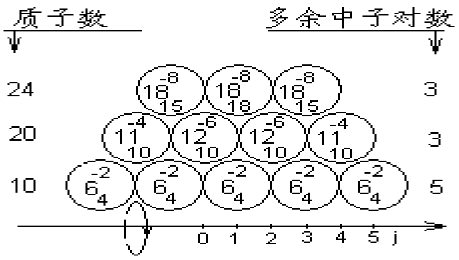

图 12.8 $^{130}_{54}Xe$ 原子核内核子、净剩 $\pi^{\pm}$ 介子分配示意图

$$Va_{4} \quad Vb^{4}_{-2} \quad Vc^{2}_{8} \quad Vd^{10}_{-4} \quad Ve^{6}_{8} \quad Vf^{14}_{-4}$$

$$Vg^{10}_{20} \quad Vh^{30}_{-12} \quad Vi^{18}_{20} \quad Vj \quad Vk^{38}_{-8} \quad Vl$$

$$Vm^{30}_{18} \quad Vn^{48}_{30} \quad Vo^{78}_{-8} \quad Vp \quad Vq^{70}_{-16}$$

$$W_e = 7.926277014\times10^{-28}Kg$$

$$W_b = 1.614707866\times10^{-29}Kg$$

$$\sum {}^{130}_{54}XeW_1 = 2.15663905\times10^{-25}Kg$$

$^{130}_{54}Xe$ Nucleus kernel force balance to verify results (figure 12.8, unit: N) table 12.10

j / N_a	1	2	3 6	4	5	nuclearElectric and magnetic field force accumulated	
34 $F_{e\theta}$ $F_{b\theta}$		q. 1170.054522 -1222.642839				↑	
16 $F_{e\theta}$ $F_{b\theta}$	h. 361.9599434 -943.7382342	k. 1008.949365 -629.1588228				|	1009.829894
$F_{e\theta}$ 34/13 $F_{b\theta}$ $\Delta F_{\theta b}$		d. 712.7489433 -57.06223088	f. 307.2004698 -57.06223088 -275.7855997			||	630.0393516

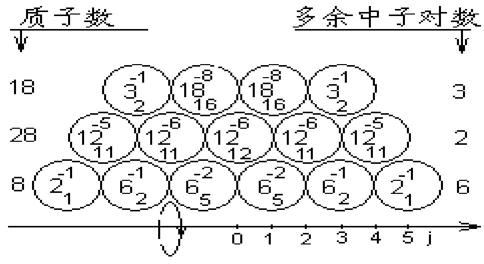

图 12.9 ${}^{130}_{54}Xe$ 原子核内核子、净剩 $\pi^{\pm}$ 介子分配示意图

$$Va_{10}\quad Vb^{10}_{-4}\quad Vc^{6}_{4}\quad Vd^{10}_{-2}\quad Ve^{8}_{12}\quad Vf^{20}_{-6}$$

$$Vg^{14}_{2}\quad Vh^{16}_{22}\quad Vi^{38}_{-2}\quad Vj^{36}_{-12}\quad Vk^{24}_{22}\quad Vl^{46}_{32}$$

$$Vm^{78}_{-10}\quad Vn^{68}_{-16}\quad Vo^{52}_{4}\quad Vp^{56}_{-2}$$

$$W_e = 8.136574665 \times 10^{-28}\,Kg$$

$$W_b = 9.346342627 \times 10^{-30}\,Kg$$

$$\sum {}^{130}_{54}XeW_2 = 2.15663237 \times 10^{-25}\,Kg$$

With the table 12.2, uneven distribution of electric and magnetic field force in the nuclear, especially the bottom, not set edge of particles spiral ring, this kind of type A nucleus is still not stable. So, we should adopt the type B nuclei model to "assemble" ${}^{130}_{54}Xe$ series nuclide atom, see figure 12.9 and table 12.11.

${}^{130}_{54}$Xe nucleus kernel force balance to verify results (figure 12.9, unit: N) table 12.11

j / N_a	1	2	3	4	5		nuclearElectric and magnetic field force accumulated
34 $F_{e\theta}$ $F_{b\theta}$	n. 758.3212815 -1222.642839		p. 162.9632036 -152.8303549			↑	-316.36408
16 $F_{e\theta}$ $F_{b\theta}$		j. 917.0025056 -943.7382342		m. 359.6684459 -786.448285		|	-326.4969287
$F_{e\theta}$ 34/13 $F_{b\theta}$ $\Delta F_{\theta b}$	b. 642.7725138 -57.06223088 -306.4284441		d. 237.204948 -28.53111544 -160.8749332		i. - 162.8141647 -14.26555772 -22.98213331	|	127.0188825

12.2.3 ${}^{131}_{54}$Xe nucleus internal structure and parameter calculation

${}^{131}_{54}$Xe nucleus, the experiment measured strength value of 0.69066 U_p, electric quadrupole moment for $-0.12\times10^{-24}cm^2$. Refer to section 7.2 (12.1) and type of magnetic synthesis principle. By figure 7.4 shows, still take a, d, d, its magnetic synthesis formula is:

$$\sum U = 5U^{+}_{g1} + U^{+}_{d2} + 3U^{-}_{d2} + U^{-}_{d3} \qquad (12.3)$$

${}^{131}_{54}$Xe nucleus kernel force balance to verify results (figure 12.10, unit: N) table 12.12

j / Na	1	2	3	4	5		nuclearElectric and magnetic field force accumulated
34 Feθ Fbθ	n. 663.5682269 -687.7365970		p. 294.3919560 -401.1796816			↑	-160.7918113

16 Feθ Fbθ		j. 1028.200151 -943.7382342	m. 308.1758925 -943.7382342			-54.00408574
Feθ 34/13 Fbθ ΔFθb	b. 520.2435589 -14.26555772 -107.2499554	d. 473.2387324 -14.26555772 -191.5177776	i.–78.21443493 -14.26555772 -76.60711103			497.0963392

Will each layer in the table 9.1 net with $\pi^{\pm}$muon original strength value generation into (12.3), too: $\sum U = 0.67806 U_p$.

Similarly, according to this kind of alone m_n + 2 m_p "decentralized" $\pi^{\pm}$ mesons in (12.3) of the scheme, the $\overline{m}_{di}$,$\overline{m}_{gi}$, in table 9.1, alone the m_n +2m_p its total quality increment is: $\triangle m=1.9707240905\times10^{-29}$Kg . So, according to (12.2), ${}^{173}_{70}$Yb nuclear magnetic moment, internal structure and parameter calculation, assembly of type B ${}^{131}_{54}$Xe nucleus is shown in figure 12.10, the nuclear force balance test results shown in table 12.12.

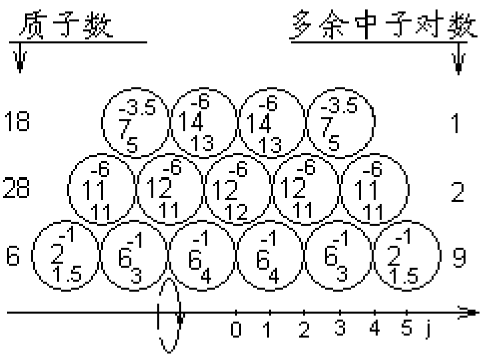

图 12.10 ${}^{131}_{54}Xe$ 原子核内核子、净剩 $\pi^{\pm}$ 介子分配示意图

$$\underset{8}{Va}\quad \overset{8}{\underset{-2}{Vb}}\quad \overset{6}{\underset{6}{Vc}}\quad \overset{12}{\underset{-2}{Vd}}\quad \overset{10}{\underset{12}{Ve}}\quad \overset{22}{\underset{-6}{Vf}}$$

$$\overset{16}{\underset{3}{Vg}}\quad \overset{19}{\underset{22}{Vh}}\quad \overset{41}{\underset{-2}{Vi}}\quad \overset{39}{\underset{-12}{Vj}}\quad \overset{27}{\underset{22}{Vk}}\quad \overset{49}{\underset{26}{Vl}}$$

$$\overset{75}{\underset{-12}{Vm}}\quad \overset{63}{\underset{-12}{Vn}}\quad \overset{51}{\underset{10}{Vo}}\quad \overset{61}{\underset{-7}{Vp}}$$

$$W_e = 8.186479798\times10^{-28} Kg$$

$$W_b = 1.086864991\times10^{-29} Kg$$

$$\sum {}^{131}_{54}XeW_1 = 2.173277665\times10^{-25} Kg$$

12.2.4 ${}^{124}_{54}$Xe nucleus internal structure and parameter calculation

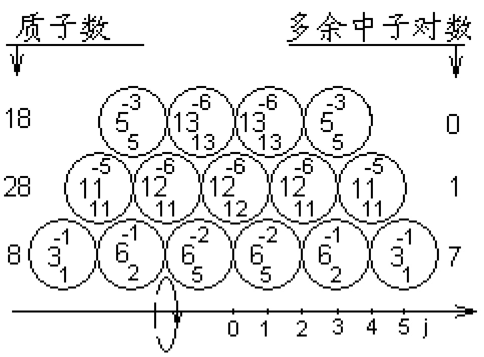

图 12.11 ${}^{124}_{54}Xe$ 原子核内核子、净剩 $\pi^{\pm}$ 介子分配示意图

$$\underset{10}{Va}\quad \overset{10}{\underset{-4}{Vb}}\quad \overset{6}{\underset{4}{Vc}}\quad \overset{10}{\underset{-2}{Vd}}\quad \overset{8}{\underset{12}{Ve}}\quad \overset{20}{\underset{-6}{Vf}}$$

$$\overset{14}{\underset{2}{Vg}}\quad \overset{16}{\underset{22}{Vh}}\quad \overset{38}{\underset{-2}{Vi}}\quad \overset{36}{\underset{-12}{Vj}}\quad \overset{24}{\underset{22}{Vk}}\quad \overset{46}{\underset{26}{Vl}}$$

$$\overset{72}{\underset{-10}{Vm}}\quad \overset{62}{\underset{-12}{Vn}}\quad \overset{50}{\underset{10}{Vo}}\quad \overset{60}{\underset{-6}{Vp}}$$

$$W_e = 8.048187241\times10^{-28} Kg$$

$$W_b = 9.346342627\times10^{-30} Kg$$

$$\sum {}^{124}_{54}XeW_1 = 2.057054499\times10^{-25} Kg$$

${}^{124}_{54}Xe$ Nucleus kernel force balance to verify results (Figure12.11 units: N) table 12.13

j / N_a	1	2	3	4	5		nuclearElectric and magnetic field force accumulated
34 Feθ Fbθ	n. 621.0364816 -687.7365970		p. 347.3510529 -343.8682985			↑	-183.5991077
16 Feθ Fbθ		j. 917.0025056 -943.7382342		m. 499.0835125 -786.4485285		|	-187.0818621
Feθ 34/13 Fbθ ΔFθb	b. 642.7725138 -57.06223088 -306.4284441		d. 237.204948 -28.53111544 -160.8749332		i. -162.8141647 -14.26555772 -22.98213331	|	127.0188825

12.2.5 $^{136}_{54}$Xe nucleus internal structure and parameter calculation

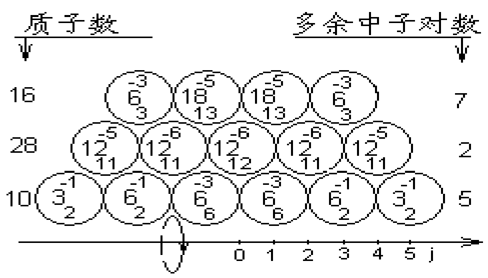

图 12.12 $^{136}_{54}Xe$ 原子核内核子、净剩 $\pi^{\pm}$

介子分配示意图

$$\underset{12}{Va}\quad \overset{12}{\underset{-6}{Vb}}\quad \overset{6}{\underset{4}{Vc}}\quad \overset{10}{\underset{-2}{Vd}}\quad \overset{8}{\underset{12}{Ve}}\quad \overset{20}{\underset{-6}{Vf}}$$

$$\overset{14}{\underset{4}{Vg}}\quad \overset{18}{\underset{22}{Vh}}\quad \overset{40}{\underset{-2}{Vi}}\quad \overset{38}{\underset{-12}{Vj}}\quad \overset{26}{\underset{22}{Vk}}\quad \overset{48}{\underset{26}{Vl}}$$

$$\overset{74}{\underset{-10}{Vm}}\quad \overset{64}{\underset{-10}{Vn}}\quad \overset{54}{\underset{6}{Vo}}\quad \overset{60}{\underset{-6}{Vp}}$$

$$W_e = 8.384428902\times10^{-28}Kg$$

$$W_b = 1.384307482\times10^{-29}Kg$$

$$\sum {}^{136}_{54}XeW_1 = 2.256337456\times10^{-25}Kg$$

$^{136}_{54}Xe$ Nucleus kernel force balance to verify results (Figure12.12 units: N) table 12.14

j / N_a	1	2	3	4	5		nuclearElectric and magnetic field force accumulated
34 $F_{e\theta}$ $F_{b\theta}$	n. 693.8586526 -477.5948590		p. 74.75470508 -286.5569154			↑	45.44894326
16 $F_{e\theta}$ $F_{b\theta}$		j. 991.1342691 -943.7382342		m. 570.0909716 -786.4485285		|	40.98735998
$F_{e\theta}$ 34/13 $F_{b\theta}$ $\Delta F_{\theta b}$	b. 792.5301253 -128.3900195 -413.6783996		d. 237.204948 -42.79667316 -137.8927999		i. -13.81634162 -14.26555772 -68.94639993		209.948882

See from the table above, the lateral force in general is slightly less than nuclear power. When we consider the first layer side by side low-energy particles spiral ring rail tangent and near because of the spin direction current yuan interval is small, with the integral method to calculate the overall ampere force will increase, as shown in the (10.20), table 10.4, may be affirmed, the nucleus is still stable, (the same below).

12.3 $^{56}_{26}Fe$, $^{40}_{20}Ca$, $^{16}_{8}O$ The nucleus and stable isotopes The internal structure and parameter calculation

12.3.1 $^{56}_{26}Fe$ nucleus and stable isotope internal structure and parameter calculation

$^{56}_{26}Fe$ nuclide and stable isotopes of 5 kinds of K_{a2} layer electronic ionization energy K_{a2} = 6390 ev, generation of (11.1) in type, too: $\sum W_{me}=2.961715803\times10^{-31}$Kg . According to the atomic energy, computing parameters to showed in table 12.15.

$^{56}_{26}Fe$ Nucleus and stable isotopes parameter experimental data results table 12.15

Nuclide	The determination of total energy atomic u	Abundance %	Nucleus total energy calculated value $\times10^{-26}$Kg	Net with $\pi\pm$ source electromagnetic field total energy $\times10^{-28}$Kg	Magnetic moment UP
$^{54}_{26}Fe$	53.9396120	5.8	8.954550586	3.250500278	
$^{56}_{26}Fe$	55.9349339	91.7	9.285881808	3.339009277	0.0902
$^{57}_{26}Fe$	56.9353907	2.19	9.452011682	3.429689989	
$^{58}_{26}Fe$	57.9332745	0.31	9.617714298	3.477645002	

We first to type A nucleus model to "assemble" $^{56}_{26}Fe$ nucleus, see figure 12.13, $^{56}_{26}Fe$ nuclear force balance verification calculation shown in table 12.16. From figure 12.13 shows: in nuclear magnetic moment = 0, under the premise of nuclear in net with $\pi^{\pm}$mesons, each layer nuclear number no further can be adjusted. At this time, we can adjust the pairs of high or low $\pi^{\pm}$mesons in each layer of particles spiral ring number of distribution. According to table 9.1 each layer $\overline{m}_{di}$,$\overline{m}_{gi}$, differences in values, see table 13.3 the calculated value of also can rise to adjust the nucleus of the total energy of function.

$^{56}_{26}Fe$ maintenance nucleus kernel force balance to verify the results table (figure 12.13, the unit: Newton)

table 12.16

j / N_a	1	2	3	4	5	nuclearElectric and magnetic field force accumulated
16 $F_{e\theta}$ $F_{b\theta}$	h. 484.0435425 -943.7382342					↑
$F_{e\theta}$ 34/13 $F_{b\theta}$ $\Delta F_{\theta b}$		d. 1257.573065 -85.59334632 -536.2497772				| 635.7299415

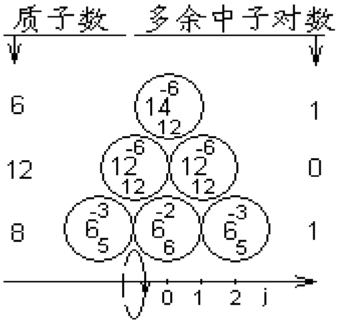

图 12.13 $^{56}_{24}Fe$ 原子核内核子、净剩 $\pi^{\pm}$ 介子分配示意图

Va_{6} $\quad Vb^{6}_{-2}$ $\quad Vc^{4}_{10}$ $\quad Vd^{14}_{-6}$ $\quad Ve$ $\quad Vf$

Vg^{8}_{24} $\quad Vh^{32}_{-12}$ $\quad Vi$ $\quad Vj$ $\quad Vk$ $\quad Vl$

Vm^{20}_{12} $\quad Vn$ $\quad Vo^{32}_{-6}$

$$W_e = 2.892590098 \times 10^{-28} Kg$$

$$W_b = 1.700296422 \times 10^{-29} Kg$$

$$\sum {}^{56}_{26}FeW_1 = 9.283813975 \times 10^{-26} Kg$$

Train to $\overline{m}^{\pm}_{d1} \rightarrow \overline{m}^{\pm}_{d2}, \overline{m}^{\pm}_{g2} \rightarrow \overline{m}^{\pm}_{g1}$, the $\sum \triangle m$ = 2.05555632 x 10^{-29} kg. After adjusting $^{56}_{26}$Fe nucleus total energy for $\sum {}^{56}_{26}$Fe W_2 =9.285869531×10^{-26}Kg, coincided with experimental value. But by shown in table 12.16, 1 layer particles spiral ring in the nuclear field force far outweigh the magnetic field, the second layer of the magnetic field strength is big, but the first layer of the lateral particle spiral ring doesn't set stability, so the nucleus is also does not exist.

When we use type B nuclei model to "assemble" $^{56}_{26}$Fe nucleus, see figure 12.14 and table 12.17. Although nuclear power field force is greater than the nuclear magnetic force, but it's better than figure 12.13 and table 12.16 shows the type A much more stable nucleus.

Of course, we also can consider to increase the layer 3 particles spiral rings, and the first layer of particles spiral ring number of protons to 10. Interested readers can do it yourself "assembly", simulated calculation exercises.

To make AA $2\overline{m}^{\pm}_{d1} \rightarrow 2\overline{m}^{\pm}_{d2}$, the $\pi^{\pm}$ source energy increment processed $\triangle$m = 1.76190544×10^{-29}Kg, for type B nucleus $^{56}_{26}$Fe after the adjustment the total energy $\sum {}^{56}_{26}$Fe W_4=9.285944876×10^{-26}Kg.

If maintain figure 12.14, $^{56}_{26}$Fe within the nucleus of the net with $\pi^{\pm}$muon distribution state, the nuclear net with $\pi^{\pm}$muon electric and magnetic field total energy and nuclear force equilibrium constant, as shown in the table 12.17. $^{58}_{26}$Fe nucleus, shillings a neutron into the first layer particles spiral ring, then to:

$$\overline{m}^{\pm}_{g2} \rightarrow \overline{m}^{\pm}_{g1}, \text{ 则} \sum {}^{58}_{26}\text{Fe } W_1 = 9.617565612 \times 10^{-26}\text{Kg} \text{ 。}$$

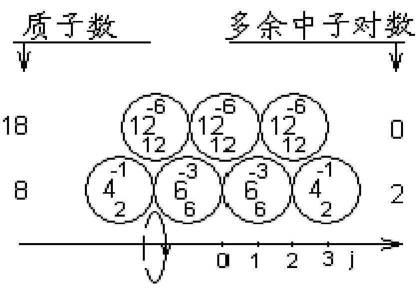

图 12.14 $^{56}_{26}Fe$ 原子核内核子、净剩 $\pi^{\pm}$介子分配示意图

Va_{12} $\quad Vb^{12}_{-6}$ $\quad Vc^{6}_{4}$ $\quad Vd^{10}_{-2}$ $\quad Ve^{8}_{12}$ $\quad Vf^{20}_{-6}$

Vg $\quad Vh^{14}_{24}$ $\quad Vi$ $\quad Vj^{38}_{-12}$

$$W_e = 3.039936250 \times 10^{-28} Kg$$

$$W_b = 1.291892102 \times 10^{-29} Kg$$

$$\sum {}^{56}_{26}FeW_3 = 9.28418297 \times 10^{-26} Kg$$

${}^{56}_{26}$Fe nucleus kernel force balance to verify results (figure 12.14, unit: N) table 12.17

j / N_a	1	2	3	4	5	nuclearElectric and magnetic field force accumulated
16 $F_{e\theta}$ $F_{b\theta}$		j. 949.7761591 -943.7382432				↑ 244.0687062
$F_{e\theta}$ 34/13 $F_{b\theta}$ $\Delta F_{\theta b}$	b. 792.5301253 -128.3900195 -413.6783998	d. 237.204948 -42.79667316 -206.8391998				| 238.0307813

Similarly, ${}^{54}_{26}$Fe nucleus, as long as in the figure 12.14 1 layer particles spiral ring in the edge of the two neutron take out, then to $\overline{m}^{\pm}_{d2} \rightarrow \overline{m}^{\pm}_{d1}$, the $\sum {}^{54}_{26}$Fe W_1 =8.95461779×10^{-26}Kg . These parameters and the experimental results are very close.

12.3. 2 ${}^{40}_{20}$Ca nucleus and stable isotope internal structure and parameter calculation

${}^{40}_{20}$Ca nuclide and stable isotopes are 5 kinds of atoms. K_{a2} layer electronic ionization energy K_{a2}=3688 ev, generation of (11.1) in type, too: $\sum W_{me}$=$1.314892005\times10^{-31}$Kg. According to the atomic energy, computing parameters to showed in table 12.18.

${}^{40}_{20}$Ca nucleus and stable isotopes parameter experimental data results table 12.18

Nuclide	The determination of total energy atomic u	Abundance %	Nucleus total energy calculated value $\times10^{-26}$Kg	Net with $\pi\pm$ source electromagnetic field total energy $\times10^{-28}$Kg	Magnetic moment UP
${}^{40}_{20}Ca$	39.9625921	96.94	6.634140339	2.521768481	
${}^{42}_{20}Ca$	41.9586281	0.65	6.965590141	2.622135397	
${}^{43}_{20}Ca$	42.9587774	0.14	7.131668953	2.707709949	-1.31721
${}^{44}_{20}Ca$	43.9554875	2.08	7.297176671	2.736175201	
${}^{46}_{20}Ca$	45.953689	0.003	7.628986063	2.872501116	

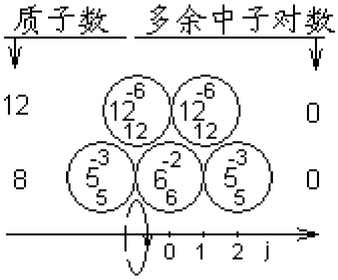

图 12.15 ${}^{40}_{20}Ca$ 原子核内核子、净剩 $\pi^{\pm}$介子分配示意图

$\underset{6}{Va}\quad \overset{6}{\underset{-2}{Vb}}\quad \overset{4}{\underset{10}{Vc}}\quad \overset{14}{\underset{-6}{Vd}}\quad Ve\quad Vf$

$\overset{8}{\underset{24}{Vg}}\quad \overset{32}{\underset{-12}{Vh}}$

$$W_e = 2.216685332\times10^{-28}\,Kg$$

$$W_b = 1.698237985\times10^{-29}\,Kg$$

$$\sum {}^{40}_{20}CaW_1 = 6.632787745\times10^{-26}\,Kg$$

We use first type A nucleus model to "assemble" ${}^{40}_{20}Ca$ nucleus. Because of equal number of protons, neutrons, we have no choice, only in 12.15 "assembly" ${}^{40}_{20}Ca$ nucleus, and make $2\overline{m}^{\pm}_{g2} \rightarrow 2\overline{m}^{\pm}_{g1}$, $\overline{m}^{\pm}_{d2} \rightarrow \overline{m}^{\pm}_{d1}$,to:

$\sum {}^{40}_{20}Ca$ W_2 = 6.634256 x 10^{-26} kg.

Although agreement with experimental data, and figure 12.13 and table 12.16 types A ${}^{56}_{26}$Fe nucleus, 1, 2 layer particles spiral ring nuclear force parameters in exactly the same, so the nucleus is still unstable or does not exist.

When we use type B "assembly" ${}^{40}_{20}Ca$ nucleus, nucleus model is shown in figure 12.16 and table 12.19.

To make $3\overline{m}^{\pm}_{d1} \rightarrow 3\overline{m}^{\pm}_{d2}$, too: $\sum {}^{40}_{20}Ca$ W_3 = 6.634091126 x 10^{-26} kg

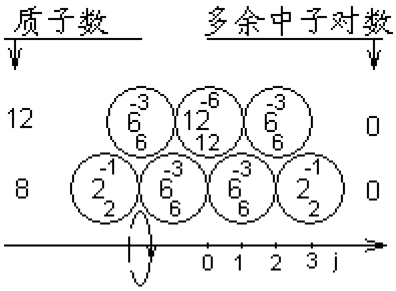

图 12.16 ${}^{40}_{16}Ca$ 原子核内核子、净剩 $\pi^{\pm}$介子分配示意图

$\underset{12}{Va}\quad \overset{12}{\underset{-6}{Vb}}\quad \overset{6}{\underset{4}{Vc}}\quad \overset{10}{\underset{-2}{Vd}}\quad \overset{8}{\underset{12}{Ve}}\quad \overset{20}{\underset{-6}{Vf}}$

$Vg\quad \overset{14}{\underset{12}{Vh}}\quad Vi\quad \overset{26}{\underset{-6}{Vj}}$

$$W_e = 2.126232534\times10^{-28}\,Kg$$

$$W_b = 1.263288342\times10^{-29}\,Kg$$

$$\sum {}^{40}_{20}CaW_2 = 6.631448268\times10^{-26}\,Kg$$

To maintain figure 12.16, the net in ${}^{40}_{20}Ca$ nucleus with $\pi^{\pm}$both scheme is changeless, adjust new neutron and high in pairs, low-energy $\pi^{\pm}$violation to the distribution of the levels, we can make the simulation ${}^{40}_{20}Ca$ isotopes, the internal structure and parameters of at this time, the nuclear spin direction of electric and magnetic energy, the nuclear force equilibrium state is unchanged.

${}^{40}_{20}Ca$ Nucleus kernel force balance to verify results (figure 12.16, unit: N) table 12.19

j / N_a	1	2	3	4	5	nuclearElectric and magnetic field force accumulated
16 $F_{e\theta}$ $F_{b\theta}$		j. 387.8536809 -471.8691171				↑ 154.0153451
$F_{e\theta}$ 34/13 $F_{b\theta}$ $\Delta F_{\theta b}$	b. 792.5301253 -128.3900195 -413.6783996		d. 237.204948 -42.79667316 -206.8391998			238.0307813

To $^{42}_{20}$Ca atomic nuclide, make a new pair of neutron into the layer 2 particles spiral ring, is:

$$\sum {}^{42}_{20}\text{CaW}_1=6.963362655\times10^{-26}\text{Kg}$$

To $2\overline{m}^{\pm}_{g2} \rightarrow 2\overline{m}^{\pm}_{g1}$, to: $\sum^{42}_{20}\text{CaW}_2 = 6.965711862 \text{ x } 10^{-26}$ kg

To $^{44}_{20}$Ca atomic nuclide, make 2 to new neutrons are into the layer 2 particles spiral ring, is:

$$\sum {}^{44}_{20}\text{CaW}_1=7.295277042\times10^{-26}\text{Kg}$$

To $\overline{m}^{\pm}_{d1} \rightarrow \overline{m}^{\pm}_{d2}$, $\overline{m}^{\pm}_{g2} \rightarrow \overline{m}^{\pm}_{g1}$, the $\sum^{44}_{20}\text{CaW}_2=7.297332599\times10^{-26}\text{Kg}$

To $^{46}_{20}$Ca atomic nuclide, make 3 to add neutron full into the layer 2 particles spiral ring, is:

$$\sum {}^{46}_{20}\text{CaW}_1=7.62719143\times10^{-26}\text{Kg}$$

And then to $2\overline{m}^{\pm}_{d1} \rightarrow 2\overline{m}^{\pm}_{d2}$, to: $\sum^{46}_{20}\text{CaW}_2 = 7.628953335 \text{ x } 10^{-26}$ kg

Synthesis of $^{43}_{20}$Ca nucleus, magnetic or in figure 7.4 a, c, d or b, d, d, by (7.6 1) type, to:

$$\sum U = U^{+}_{g1} + U^{-}_{g1} + 3U^{+}_{g2} + 2U^{+}_{d2} + 3U^{-}_{d1} \qquad (12.4)$$

$^{43}_{20}$Ca nucleus kernel force balance to verify results (figure 12.17, unit: N) table 12.20

j / N_a	1	2	3	4	5	nuclearElectric and magnetic field force accumulated
16 $F_{e\theta}$ $F_{b\theta}$		j. 433.3100386 -209.7196076				↑ 227.5599386
$F_{e\theta}$ 34/13 $F_{b\theta}$ $\Delta F_{\theta b}$	b. 792.5301253 -128.3900195 -517.0979995		d. 67.33868407 -106.9916829 -103.4195999			3.969507647

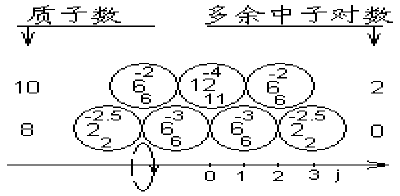

图 12.17 $^{43}_{16}Ca$ 原子核内核子、净剩 $\pi^{\pm}$介子分配示意图

$$\underset{12}{Va} \quad \overset{12}{\underset{-6}{Vb}} \quad \overset{6}{\underset{4}{Vc}} \quad \overset{10}{\underset{-5}{Vd}} \quad \overset{5}{\underset{11}{Ve}} \quad \overset{16}{\underset{-4}{Vf}}$$

$$Vg \quad \overset{12}{\underset{12}{Vh}} \quad Vi \quad \overset{24}{\underset{-4}{Vj}}$$

$$W_e = 2.023653299 \times 10^{-28} Kg$$

$$W_b = 1.263917481 \times 10^{-29} Kg$$

$$\sum {}^{43}_{20}CaW_1 = 7.12814786 \times 10^{-26} Kg$$

Will the original magnetic strength values in table 9.1 generation into (12.4), too: $\sum U = -1.26551 U_p$. Similarly, quality increment is: train $\triangle m$ = -8.80952673 x 10^{-30} kg

"Assembly" $^{43}_{16}Ca$ nucleus figure 12.17, the nuclear force balance test results shown in table 12.20.

To $3\overline{m}^{\pm}_{g2} \rightarrow 3\overline{m}^{\pm}_{g1}$,to: $\sum^{43}_{20} CaW_2$ = 7.131671671 x 10^{-26} kg

12.3.3 $^{16}_{8}$O nuclei and stable isotope internal structure and parameter calculation

$^{16}_{8}$O atom nuclide is only 3 and stable isotopes. K_{a2} layer electronic ionization energy K_{a2}=523 ev, generation of (11.1) in type, to:$\sum W_{me}$=41804ev=7.45866×10^{-33}Kg. Calculated according to the atomic energy, energy parameters to showed in table 12.21.

$^{16}_{8}$O nuclei and stable isotopes energy parameters experimental data, the results table table 12.21

Nuclide	The determination of total energy atomic u	Abundance %	Nucleus total energy calculated value $\times 10^{-26}$Kg	Net with π± source electromagnetic field total energy $\times 10^{-28}$Kg	Magnetic moment U_P
$^{16}_{8}O$	15.99491502	99.76	2.655291933	1.172287172	
$^{17}_{8}O$	16.9991333	0.039	2.822046416	1.325428772	-1.89371
$^{18}_{8}O$	17.99915996	0.205	2.988104863	1.408966837	

We first to type A nucleus model "assembly" $^{16}_{8}$O nuclei, see figure 12.18 and table 12.22.

$^{16}_{8}$O nuclei kernel force balance test results list (figure 12.18, unit: N) table 12.22

j / N_a	1	2	3	4	5	nuclearElectric and magnetic field force accumulated
$F_{e\theta}$		d. 1257.573065				↑ 635.7299417
34/13 $F_{b\theta}$		-85.59334632				|
$\Delta F_{\theta b}$		-536.24977762				|

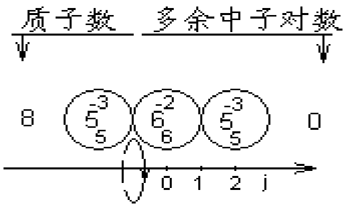

$$W_e = 9.560477373 \times 10^{-29}\,Kg$$
$$W_b = 1.689408034 \times 10^{-29}\,Kg$$
$$\sum {}^{16}_{8}OW_1 = 2.654818947 \times 10^{-26}\,Kg$$

图 12.18 ${}^{16}_{8}O$ 原子核内核子、净剩

$\pi^{\pm}$介子分配示意图

$$\underset{6}{Va} \quad \overset{6}{\underset{-2}{Vb}} \quad \overset{4}{\underset{10}{Vc}} \quad \overset{14}{\underset{-6}{Vd}}$$

Can be seen from the above results is that ${}^{16}_{8}$O conditions within the nucleus net with $\pi^{\pm}$violation can such distribution, and nuclear power, magnetic field is a maximum total energy, nuclear energy, but still less than the value, the nuclear force is also unable to balance. So, A type ${}^{16}_{8}$O nuclear model also cannot exist.

Similarly, "assembly" type B ${}^{16}_{8}$O nucleus figure 12.19, the nuclear force balance verification calculation shown in table 12.23.

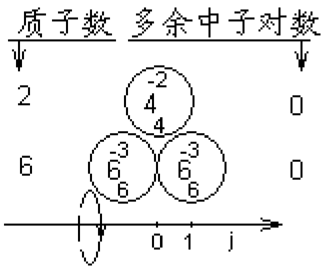

$$\overset{12}{\underset{12}{Va}} \quad \overset{12}{\underset{-6}{Vb}} \quad Vc \quad Vd \quad \overset{6}{\underset{4}{Ve}} \quad \overset{10}{\underset{-2}{Vf}}$$

$$W_e = 9.10194656 \times 10^{-29}\,Kg$$
$$W_b = 1.379237908 \times 10^{-29}\,Kg$$
$$\sum {}^{16}_{8}OW_1 = 2.654050246 \times 10^{-26}\,Kg$$

图 12.19 ${}^{16}_{8}O$ 原子核内核子、净剩

$\pi^{\pm}$介子分配示意图

${}^{16}_{8}$O nuclei kernel force balance test results list (figure 12.19, unit: N) table 12.23

j / N_a	1	2	3	4	5	nuclearElectric and magnetic field force accumulated
$F_{e\theta}$ 34/13 $F_{b\theta}$ $\Delta F_{\theta b}$		b. 792.5301253 -128.3900195 -620.5175993				↑ 43.62250648

Make to $\overline{m}_{g2}^{\pm} \rightarrow \overline{m}_{g1}^{\pm}$, to: $\sum {}^{16}_{8}OW_2 = 2.65522486 \times 10^{-26}$Kg

To ${}^{18}_{8}$O nuclei, and make a pair of neutron into layer, layer 2 particles spiral ring:

$$\sum {}^{18}_{8}OW_1 = 2.985964633 \times 10^{-26}\text{Kg}$$

To make $\overline{m}_{g2}^{\pm} \rightarrow \overline{m}_{g1}^{\pm}$, $\overline{m}_{d1}^{\pm} \rightarrow \overline{m}_{d2}^{\pm}$, to: $\sum{}^{18}_{8}OW_2 = 2.98802019\times10^{-26}Kg$

Synthesis of ${}^{17}_{8}O$ nuclei, magnetic take in figure 7.4 a, d, d, by (7.6-4) and table 9.1 data:

$$\sum U = 5U_{g1}^{+} + 2U_{d1}^{-} + U_{d2}^{+} + 2U_{d2}^{-} = -1.93864U_p \qquad (12.5)$$

$$\Delta m = 1.321429084\times10^{-29}Kg$$

Its internal structure and the calculation result is shown in figure 12.20 and table 12.24.

To make $\overline{m}_{g1}^{\pm} \rightarrow \overline{m}_{g2}^{\pm}$, $\overline{m}_{d1}^{\pm} \rightarrow \overline{m}_{d2}^{\pm}$, to: $\sum{}^{17}_{8}OW_2 = 2.82206546\times10^{-26}Kg$

${}^{17}_{8}O$ nuclei kernel force balance test results list (figure 12.20, unit: N) table 12.24

j / N_a	1	2	3	4	5	nuclearElectric and magnetic field force accumulated
$F_{e\theta}$ 34/13 $F_{b\theta}$ $\Delta F_{\theta b}$		b. 986.8248433 -128.3900195 -766.0711103				↑ 92.36371348

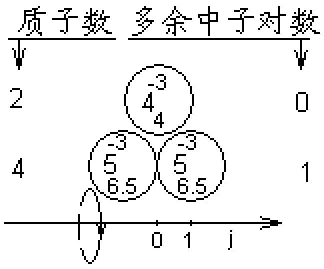

$$\underset{13}{\overset{}{Va}} \quad \underset{-6}{\overset{13}{Vb}} \quad Vc \quad Vd \quad \underset{4}{\overset{7}{Ve}} \quad \underset{-3}{\overset{11}{Vf}}$$

$$W_e = 1.061847095\times10^{-28}Kg$$
$$W_b = 1.62708268\times10^{-29}Kg$$
$$\sum{}^{17}_{8}OW_1 = 2.822359111\times10^{-26}Kg$$

图 12.20 ${}^{17}_{8}O$ 原子核内核子、净剩 $\pi^{\pm}$介子分配示意图

Through the chapter 11, 12 of several nuclei and isotope internal model design, the nuclear force balance test simulation results, we can see that: the number of nuclear A≥12 all the nucleus, nucleus is B, internal nuclear force to balance. Because each layer particles spiral ring high and low $\pi^{\pm}$ violation of, neutron energy fluctuation in the original slightly difference, in neighbouring particles spiral ring in motivating, transition does not affect the distribution of nuclear power, but it can reflect the total energy of the nucleus, it is without the γ rays, x rays, formation conditions, nuclear small changes in the internal energy and nuclear power.

12.4 Light nuclei supplement internal structure and Parameter calculation

12.4.1 Light $N_{\alpha di}$、$N_{\alpha gi}$、$\overline{M}_{di}$、$\overline{M}_{gi}$ added calculation parameters within the nucleus

Front chapter 7 of section 7.1 shown in figure 7.1 and figure 7.2, the first layer, low-energy particle spiral loop combination model with 2 ~ 5 layers. But this scheme is applicable to the quality of medium to heavy nuclei. To light nuclei and the simulation results can be seen from the previous section: common small total energy and nuclear electric field in repelling force slants big; therefore, to light nuclei, we can consider to use the first layer and 2 ~ 5 layer, low-energy particle spiral rings set combination model of the same.

Refer to chapter 8 $^{12}_{6}C\ \overline{M}_{\pi d1}$ forces within the nucleus of the benchmark constant calculation method. Shilling $N_{\alpha d1}=34/13$, and (4.9) in type $\beta_{\alpha d1}$ are obtained. Refer to chapter 9 $N_{\alpha di}$、$N_{\alpha gi}$、$\overline{M}_{di}$、$\overline{M}_{gi}$ parameter simulation calculation method, the $N_{\alpha gi}$ = 4, 5, 6 of a natural number. Respectively into (9.7) and (9.9) and (9.6) equations, get $N_{\alpha gi}$ = 5. Finally by chapter 8 section 8.4 the last 1 ~ 12 simulation procedures, simulation is obtained:

$$\overline{M}_{\pi d1}=3.572742815\times10^{-28}\text{Kg}$$

$^{56}_{26}Fe$、$^{40}_{20}Ca$、$^{16}_{8}O$ Uclei original energy simulation results ratio table table 12.25

Atomic nuclide / The project	$^{56}_{26}Fe$	$^{40}_{20}Ca$	$^{16}_{8}O$
Experimental value (10^{-26} kg)	9.285881808	6.634140339	2.655291933
Type B the simulation predicted value of the nucleus	9.28418297	6.631448286	2.654050246
The ratio of experimental data and the simulation value	1.000182982	1.000405952	1.000467846
Electromagnetic field the ratio of total energy and nuclear energy	0.0034135	0.0033968	0.0039491

Us from in front of all the particles in the nucleus of solenoid ring of surplus high and low $\pi^{\pm}$ violation, the spin direction of electromagnetic field energy accumulated in the already know, the electromagnetic field energy is always positive. Accounted for the nucleus of the total energy of 0.003 ~ 0.004, see table 12.25. When we take $N_{\alpha g1}$= 5, $N_{\alpha d1}$ = 34/13, and figure 7.1 and figure 7.2 2 ~ 5 layers of particles spiral ring of the same set of ring structure, simulation results $\overline{M}_{\pi d1}$ values being beyond 8%! Far outweigh the electromagnetic field energy, clearly obvious. So, further simulation and comparison, see table 12.26, the appropriate value is: $N_{\alpha d1}=N_{\alpha g1}$= 17/6. It can properly increase the quality of the light nuclei, and may be appropriate to reduce nuclear power field force, make the internal nuclear force equilibrium.

The first layer of particles spiral ring different quantum fluctuations benchmark constant changes $\overline{M}_{\pi d1}$

simulation result table table 12.26

$N_{\alpha d1}$ $N_{\alpha g1}$	34/13 34/13	21/8 21/8	17/6 17/6	34/13 17/6	34/13 5

$\overline{M}_{\pi d1} \times 10^{-28}$Kg	3.304461327	3.304486416	3.304966183	3.351764984	3.572742815
与原基准常数的比值	1	1.000007592	1.00015278	1.014315089	1.081187662

Table 9.1 similarly, refer to chapter 9 nucleus of internal related parameters calculation method of the added calculation, and calculate the result of light conditions within the nucleus $N_{\alpha di}$、$N_{\alpha gi}$、$\overline{M}_{di}$、$\overline{M}_{gi}$ parameters shown in table 12.27.

Light conditions within the nucleus $N_{\alpha di}$、$N_{\alpha gi}$、$\overline{M}_{di}$、$\overline{M}_{gi}$ parameters complement the results table table 12.27

Particles spiral link layer		1	2	3
波动量子数 Quantum fluctuations number	$N_{\alpha di}$	17/6	16	34
	$N_{\alpha gi}$	17/6	50	114
$R_{\theta di(0)} / R_{\theta gi(0)}$		2	0.9882663482	0.9984184964
$\overline{M}_{di} \times 10^{-28} Kg$ $\overline{M}_{gi} \times 10^{-28} Kg$		3.304966183 6.609932366	3.349020548 6.551193213	3.325851224 6.582085645
K_{mui}		2	1.956151991	1.979067974
$U^{-}_{\pi di} \times 10^{-26}$ J/T $U^{+}_{\pi gi} \times 10^{-26}$ J/T		3.177738798 1.588869399	2.605275456 1.302637728	2.578319713 1.289159857
Neutron of surplus energy $\times 10^{-30} Kg$		0.0	14.6847884	6.9616804
$\pi^{\pm}$ Violation of transition energy $\Delta\overline{M}^{\pm}_{di} \times 10^{-30} Kg$ $\Delta\overline{M}^{\pm}_{gi} \times 10^{-30} Kg$			8.810873 11.7478306	4.6338648 6.1784864

Obtained by the same token, by (9.12), light nucleus layers particles spiral ring number of nuclear density respectively: 6, 12, 18 and 24.

12.4.2. Light nuclei internal parameters of the nuclear power field Energy supplement

Similarly, refer to section 9.2 and chapter 10 conditions within the nucleus electric energy parameters and the analysis of the electromagnetic force calculation method, added calculation for light conditions within the nucleus electric energy, the parameters of the electromagnetic force results see table 12.28 ~ 12.28.

Type A high light within the nucleus, low-energy particles spiral ring net with to $\pi^{\pm}$ mesons in potential can supplement parameter calculation table (unit: V) 12.28

$N_{\alpha di}$	$N_{\alpha gi}$ / $\overline{M}_{dgi}\times10^{-28}Kg$	0	1	2	3	4
34	3.325851224	m. 234974.3191		n. 222418.0372		
114	6.582085645	k. 252585.8481		l. 236896.8441		
16	3.349020548		h. 338009.4186		j. 279845.3358	
50	6.551193213		g. 367054.7807		i. 293535.6784	
17/6	3.304966183	b. 923649.0682		d. 604437.8209		f. 375758.6618
17/6	6.609932366	a. 1847298.136		c. 751517.3235		e. 406970.8136

Type B high light within the nucleus, low-energy particles spiral ring net with to $\pi^{\pm}$ mesons in potential can supplement parameter calculation table (unit: V) 12.29

$N_{\alpha di}$	$N_{\alpha gi}$ / $\overline{M}_{dgi}\times10^{-28}Kg$	0	1	2	3	4
34	3.325851224		j. 231636.5691			
114	6.582085645		i. 248373.0973			
16	3.349020548	f. 348163.0047		h. 312191.3818		
50	6.551193213	e. 380714.9489		g. 333494.552		
17/6	3.304966183		b. 793951.3881		c. 467932.561	
17/6	6.609932366		a. 1208875.642		d. 530611.8724	

Type A high light within the nucleus, low-energy particles spiral ring net with to $\pi^{\pm}$ mesons in electric field force parameters added calculation (unit: N) table 12.30

$N_{\alpha di}$	$N_{\alpha gi}$ / $\overline{M}_{dgi}\times10^{-28}Kg$	0	1	2	3	4
34	3.325851224	m		n. 1.749847022		
114	6.582085645	k		l. 2.156969519		
16	3.349020548		h. 2.958737819		j. 5.022909216	
50	6.551193213		g 3.940643992		i. 6.044190487	
17/6	3.304966183	b		d. 24.75830452		f. 11.41675181
17/6	6.609932366	a		c. 45.66700726		e. 14.39055243

Type B high light within the nucleus, low-energy particles spiral ring net with to $\pi^{\pm}$ mesons in electric field force parameters added calculation (unit: N) table 12.31

$N_{\alpha di}$	$N_{\alpha gi}$ / $\overline{M}_{dgi}\times10^{-28}Kg$	0	1	2	3	4

34	3.325851224		j. 0.988472504	
114	6.582085645		i. 1.242963523	
16	3.349020548	f	h. 4.655661251	
50	6.551193213	e	g. 5.910106907	
17/6	3.304966183		b. 30.20475342	c. 16.72091553
17/6	6.609932366		a. 45.66700726	d. 23.95612641

12.4.3. Light nuclei internal ring particles spiral magnetic force parameters calculation

Light conditions within the nucleus low-energy particles spiral ring current magnetic field force parameters complement the results table table 12.32

$N_{\alpha di}$ / 参数（公式）	17/6	16	34
$M_{di} \times 10^{-28} Kg$	3.304966183	3.349020548	3.325851224
β_i (4.9)	0.9989628612	0.998751741	0.9987299178
α_1° (10.5-5)	126.4476824	104.4775122	99.8749614
$K_{ri} \times 10^{-5}$ （2.10）	13.7902	6.36539	4.40105
$F_{kbi}(N)$ (10.11)	17.51945005	26.22296182	19.10963214
$K_{fbi}(N)$ (10.17)	6.796082125	0.5200280083	0.1655611159

Similarly, refer to section 9.2 and chapter 10 section 10.2 conditions within the nucleus particles spiral ring the analysis of the magnetic field strength calculation method, added calculation for light nuclei within the parameters of the magnetic field strength results shown in table 12.30.

12.5 $^{56}_{26}$Fe, $^{40}_{20}$Ca, $^{16}_{8}$O nuclei and stable isotope internal Structure and parameters calculation

12.5.1 $^{56}_{26}$Fe nucleus and stable isotope internal structure and Parameters calculation

$^{56}_{26}$Fe nucleus kernel added calculation result is proved force balance table (figure 12.21 units: Newton) of

12.33

j / N_a	1	2	3		nuclearElectric and magnetic field force accumulated （original Nuclear force parameters ）
16 $F_{e\theta}$ $F_{b\theta}$	h. 484.1914583 -944.0266255				
$F_{e\theta}$ 17/6 $F_{b\theta}$ $\Delta F_{\theta b}$		d. 1237.991278 －105.1167003 － 475.7257488		↑ |	657.148829 （635.7299415）

By in front of the results of table 12.15, we first to type A nucleus model to add "assembly" $^{56}_{26}$Fe nucleus, see figure 12.21, $^{56}_{26}$Fe nuclear force balance verification calculation shown in table 12.33.

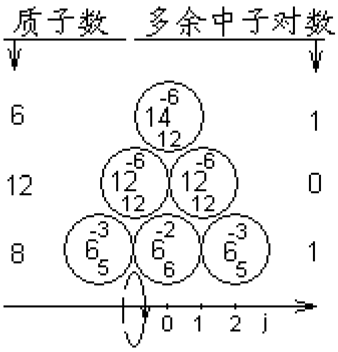

图 12.21 $^{56}_{24}Fe$ 原子核内核子、净剩 $\pi^{\pm}$ 介子分配补充示意图

$$\underset{6}{Va}\quad \overset{6}{\underset{-2}{Vb}}\quad \overset{4}{\underset{10}{Vc}}\quad \overset{14}{\underset{-6}{Vd}}\quad Ve\quad Vf$$

$$\overset{8}{\underset{24}{Vg}}\quad \overset{32}{\underset{-12}{Vh}}\quad Vi\quad Vj\quad \overset{20}{\underset{12}{Vk}}\quad Vl$$

$$\overset{32}{\underset{-6}{Vm}}\quad Vn$$

$$W_e = 2.859518388 \times 10^{-28} Kg$$

$$W_b = 1.560541023 \times 10^{-29} Kg$$

$$\sum {}^{56}_{26}FeW_1 = 9.284757205 \times 10^{-26} Kg$$

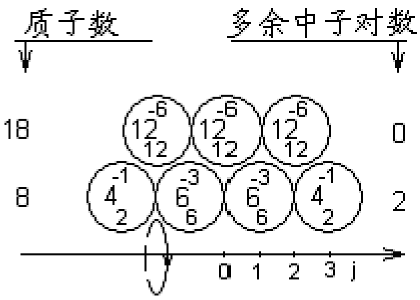

图 12.22 $^{56}_{26}Fe$ 原子核内核子、净剩 $\pi^{\pm}$ 介子补充分配示意图

$$\overset{12}{\underset{12}{Va}}\quad \overset{12}{\underset{-6}{Vb}}\quad \overset{6}{\underset{4}{Vc}}\quad \overset{10}{\underset{-2}{Vd}}\quad \overset{8}{\underset{12}{Ve}}\quad \overset{20}{\underset{-6}{Vf}}$$

$$\overset{14}{\underset{24}{Vg}}\quad \overset{38}{\underset{-12}{Vh}}$$

$$W_e = 3.019635581 \times 10^{-28} Kg$$

$$W_b = 1.192644484 \times 10^{-29} Kg$$

$$\sum {}^{56}_{26}FeW_3 = 9.285294313 \times 10^{-26} Kg$$

To $\overline{m}^{\pm}_{g2} \rightarrow \overline{m}^{\pm}_{g1}$, accidents are $\sum\Delta m$ = 11.7478306 x 10^{-30} kg. After adjusting $^{56}_{26}$Fe nucleus total energy for -$\sum^{56}_{26}FeW_2$ = 9.285931988 x 10^{-26} kg, with experimental value ratio of 1.0000054, is also very consistent. Shown by table 12.33, however, nuclear power magnetic field force of value is slightly larger than the original.

$^{56}_{26}$Fe nucleus kernel added calculation result is proved force balance table (figure 12.22 units: Newton) of 12.34

j / N_a	1 2 3 4 5				nuclearElectric and magnetic field force accumulated
16 $F_{e\theta}$ $F_{b\theta}$		h. 950.0663948 -944.0266255		↑ |	306.6174184 （244.0687062）

$F_{e\theta}$ 17/6 $F_{b\theta}$ $\Delta F_{\theta b}$	b. 828.483919 -157.6750505 -366.9884348	d. 232.8097828 -52.55835015 -183.4942174		| |	300.5776491 （238.0307813）

When we use type B nuclei model to add "assembly" $^{56}_{26}$Fe nucleus, see figure 12.22 and table 12.34.

To make $\overline{m}_{d1}^{\pm} \to \overline{m}_{d2}^{\pm}$, the $\pi^{\pm}$source energy increment Δm = 8.810873 x 10^{-30} kg, for type B nucleus $^{56}_{26}$Fe after the adjustment the total energy $\sum^{56}_{26} FeW_4$ = 9.2861754 x 10^{-26} kg.

Of course, we also can consider to increase the layer 3 particles spiral rings, and the first layer of particles spiral ring number of protons to 10. Interested readers can do it yourself "assembly", simulated calculation exercises.

If maintain figure 12.22, $^{56}_{26}$Fe within the nucleus of the net with $\pi^{\pm}$muon distribution state, the nuclear net with $\pi^{\pm}$muon electric and magnetic field total energy and nuclear force equilibrium constant, as shown in the table 12.34. $^{58}_{26}$Fe nucleus, shillings a neutron into the first layer particles spiral ring, then make: $\overline{m}_{g2}^{\pm} \to \overline{m}_{g1}^{\pm}$, then $\sum^{58}_{26} FeW_1$=9.617846802 x 10^{-26} kg.

Similarly, $^{54}_{26}$Fe nucleus, as long as in the figure 12.22 1 layer particles spiral ring in the edge of the two neutron, then $\sum^{54}_{26} FeW_1$ = 8.954797695 x 10^{-26} kg. These parameters and the experimental results are very close.

12.5.2 $^{40}_{20}$Ca nucleus supplement internal structure and parameter calculation

We first use type A nucleus model to add "assembly" $^{40}_{20}Ca$ nucleus. Because of the equal number of protons, neutrons, we have no choice, only in 12.23 "assembly" $^{40}_{20}Ca$ nucleus, and order: $\overline{m}_{d1}^{\pm} \to \overline{m}_{d2}^{\pm}$, to:

$\sum^{40}_{20}Ca\ W_2$=6.63420698 x 10^{-26} kg.

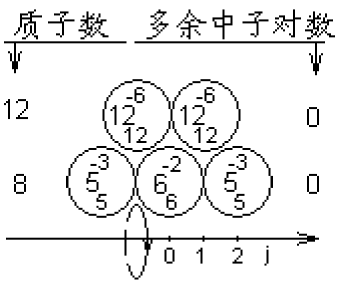

图 12.23 $^{40}_{20}Ca$ 原子核内核子、净剩 $\pi^{\pm}$介子分配补充示意图

Va_{6} $\quad Vb^{6}_{-2}$ $\quad Vc^{4}_{10}$ $\quad Vd^{14}_{-6}$ $\quad Ve$ $\quad Vf$

Vg^{8}_{24} $\quad Vh^{32}_{-12}$

$$W_e = 2.18351035 \times 10^{-28} Kg$$

$$W_b = 1.5584234 \times 10^{-29} Kg$$

$$\sum {}^{40}_{20}CaW_1 = 6.633325893 \times 10^{-26} Kg$$

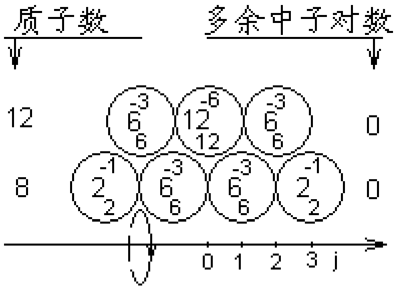

图 12.24 $^{40}_{20}Ca$ 原子核内核子、净剩

$\pi^{\pm}$介子分配补充示意图

$\overset{}{\underset{12}{Va}}\ \overset{12}{\underset{-6}{Vb}}\ \overset{6}{\underset{4}{Vc}}\ \overset{10}{\underset{-2}{Vd}}\ \overset{8}{\underset{12}{Ve}}\ \overset{20}{\underset{-6}{Vf}}$

$\overset{14}{\underset{12}{Vg}}\ \overset{26}{\underset{-6}{Vh}}\ Vi\ \ Vj$

$$W_e = 2.105792269\times10^{-28}Kg$$
$$W_b = 1.163840951\times10^{-29}Kg$$
$$\sum {}^{40}_{20}CaW_2 = 6.63215413\times10^{-26}Kg$$

Although agreement with experimental data, and figure 12.21 and table 12.33 type A $^{56}_{26}$Fe nucleus, 1, 2 layer particles spiral ring nuclear force parameters in exactly the same, so the nucleus is still unstable or does not exist.

When we use type B nuclei model added "assembly" $^{40}_{20}Ca$ nucleus, see figure 12.24 and table 12.35.

$^{40}_{20}Ca$ Added calculation result is proved nucleus kernel force balance table (figure 12.24 units: Newton) of 12.35

j / N_a	1	2	3	4	5	nuclearElectric and magnetic field force accumulated	
16 $F_{e\theta}$ $F_{b\theta}$		j. 387.9722025 －472 .0133128				↑	216.5365388 （154.0153451）
$F_{e\theta}$ 17/6 $F_{b\theta}$ $\Delta F_{\theta b}$	b. 828.483919 -157.6750505 -366.9884348		d. 232.8097828 -52.55835015 -183.4942174			|	300.5776491 （238.0307813）

To $\overline{m}^{\pm}_{d1} \rightarrow \overline{m}^{\pm}_{d2}$ $\overline{m}^{\pm}_{g2} \rightarrow \overline{m}^{\pm}_{g1}$, to: $\sum {}^{40}_{20}Ca\ W_3{=}6.63421\times10^{-26}Kg$

12.5.3 $^{16}_{8}$O nuclei supplement internal structure and parameter calculation

We first to type A nucleus model "assembly" $^{16}_{8}$O nuclei, see figure 12.25 and table 12.36.

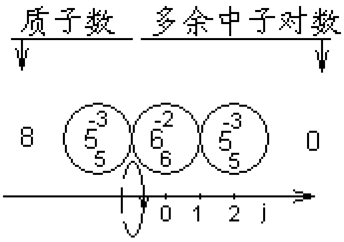

图 12.25 $^{16}_{8}O$ 原子核内核子、净剩

$\pi^{\pm}$介子分配补充示意图

$\overset{}{\underset{6}{Va}}\ \overset{6}{\underset{-2}{Vb}}\ \overset{4}{\underset{10}{Vc}}\ \overset{14}{\underset{-6}{Vd}}$

$$W_e = 9.226801614 \times 10^{-29} Kg$$
$$W_b = 1.532931683 \times 10^{-29} Kg$$
$$\sum {}^{16}_{8}OW_1 = 2.65473268 \times 10^{-26} Kg$$

${}^{16}_{8}$O nuclei kernel added calculation result is proved force balance table (figure 12.25 units: Newton) of 12.36

j / N_a	1	2	3	4	5	nuclearElectric and magnetic field force accumulated	
$F_{e\theta}$		d. 1237.991278				↑	657.1488285
17/6 $F_{b\theta}$		－105.1167003				|	（635.7299417）
$\Delta F_{\theta b}$		－475.7257488				|	

Can be seen from the above results is that ${}^{16}_{8}$O conditions within the nucleus net with $\pi^{\pm}$violation can such distribution, and nuclear power, magnetic field is a maximum total energy, nuclear energy, but still less than the value, the nuclear force is also unable to balance. So, A type ${}^{16}_{8}$O nuclear model also cannot exist.

Similarly, "assembly" type B ${}^{16}_{8}$O nucleus figure 12.26, the nuclear force balance verification calculation shown in table 12.37.

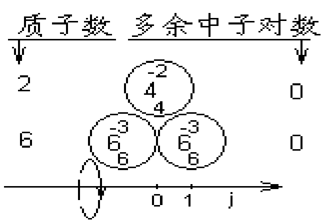

$$W_e = 8.927862779 \times 10^{-29} Kg$$
$$W_b = 1.250605562 \times 10^{-29} Kg$$
$$\sum {}^{16}_{8}OW_1 = 2.654151415 \times 10^{-26} Kg$$

图 12.26 ${}^{16}_{8}O$ 原子核内核子、净剩

$\pi^{\pm}$介子分配补充示意图

$$\underset{12}{Va} \quad \overset{12}{\underset{-6}{Vb}} \quad Vc \quad Vd \quad \overset{6}{\underset{4}{Ve}} \quad \overset{10}{\underset{-2}{Vf}}$$

To make $\overline{m}^{\pm}_{g2} \rightarrow \overline{m}^{\pm}_{g1}$， to：$\sum {}^{16}_{8}OW_2 = 2.655326198 \times 10^{-26}$Kg

Front has stressed that the parameters of the simulation in nucleus, energy conservation and nuclear force balance is two important principles. From the 12.4 and 12.5 of this chapter two within the nucleus of the related parameters of simulation results is to see that by the law of conservation of energy only allowed particles spiral loop quantum fluctuations of the first layer of $N_{\alpha g1} = N_{\alpha d1} = 17/6$, but nuclear force balance simulation results of the system increases, so, the original of the parameters of the conditions within the nucleus is the best choice.

${}^{16}_{8}$O nuclei kernel added calculation result is proved force balance table (figure 12.26 units: Newton) of 12.37

j / N_a	1	2	3	4	5	nuclearElectric and magnetic field force accumulated	
$F_{e\theta}$ 17/6 $F_{b\theta}$ $\Delta F_{\theta b}$		b. 828.483919 －157.6750505 －550.4826521				↑ | |	120.3262164 （43.62250648）

13 □Rays in nucleus forming principle and Parameter calculation

13.1 Conditions within the nucleus formation

Principle of □rays

13.1.1 $\beta^{\pm}$ Electronics and photon, neutrino associated principle

Conditions within the nucleus only have high and low $\pi^{\pm}$violation of spiral ring particles. When a $\pi^{\pm}$ split muon decay, internal 2 of charged particles and a charged particle collection divided, can be generated by a pair of charged particles and a charged particles composed of electrons, left a pair of charged particles formed neutrinos or photons. With nuclear power by the number of the same isotopes, less number of neutrons, main show is β^{+} positron emission. Along with the increased number of neutrons, transition to stable isotopes. If the neutron number to continues increase, the performance of β^{-} electron emission.

Both β^{+} or β^{-} electron emission, the total number of nuclear are the parent nucleus remain unchanged. When launching a β^{+} electronic, number of nuclear power by reducing 1, within a proton nuclear will be transformed into neutrons. By figure 7.4, protons, neutrons "decentralized" $\pi^{\pm}$source distribution graph to: particles spiral rings a high-energy π_g^{+} source must be continuously absorbs neutrinos in game 4 of neutrinos, then split decay into a pair of low-energy $\pi_d^{\pm}$ mesons, an electronic β^{+}; A low-energy $\pi_d^{\pm}$ muon to low-energy particles spiral ring rail, β^{+} positron emission form β^{+} rays, complete the protons and neutrons transformation process. Similarly, if the diffusion β^{-} launch, the mother will have a neutron nuclear into protons. At this time, as long as A low-energy π_d^{-} violation will be their most primitive wave motion direction of electromagnetic field energy transfer to another low π_d^{+} after mesons, its direct split into a β^{-} electronics and A photon or neutrinos emission; Another low π_d^{+} muon after absorbing energy is emitted into the high-energy π_g^{+} muon orbit, complete the neutrons and protons.

13.1.2 γ Rays forming principle

Conditions within the nucleus does not exist, electrons and photons neutrinos, but is a nucleus in the ubiquity of neutrino field, the neutrino through at any moment. When conditions within the nucleus by net with $\pi^{\pm}$ muon electric and magnetic field, the formation of nuclear force and energy distribution is uniform, do not need to adjust, stable, even more neutrino through nucleus, also won't produce.

When nucleus kernel force balance, not nuclear power, nuclear power by uneven distribution, to adjust itself to nuclear power, nuclear force distribution, make whole nuclei tend to be stable, the particles spiral ring net with to $\pi^{\pm}$mesons in the state of the distribution adjustment is inevitable. Net with $\pi^{\pm}$mesons in each particle spiral loop adjustment, redistribution will cause the change of electric and magnetic energy in nuclear. When it is reduces the surplus electricity, magnetic energy through stimulating through nucleus formation of neutrino photons. Such already can transfer surplus energy, and can produce γ rays. Neutron or in pairs, of course, $\pi^{\pm}$ violation in the particles spiral ring layer between the adjustment, redistribution, residual energy can also produce γ rays.

13.1.3 □Ray spectrum energy form model

From chapter 11, 12 nucleus structure calculation and analysis in the know, nature can stability of nuclide atom, the number of nuclear power by $Z_i \leq 83$. All the nucleus of $Z_i \geq 6$, nuclear power charge can be evenly distributed, the nuclear force balance without splitting the moment of the nucleus is type B nucleus. When the first layer is 6 to particles spiral ring side by side, 4 ring particles spiral layer composed of nearly spherical nuclei, saturated when the total number of nuclear is 234, and the department of radiation starting nuclear quite; When after the first layer of 4, 3 layers particles spiral loop composed of the nearly spherical nuclei saturated when the total number of nuclear is 96. So, the nuclear of $234 \geq A \geq 96$ all the nucleus, may think they have A combination of particles spiral ring structure shown in figure 13.1. The difference is that with the increase of the nuclear number, nuclear power by number, nucleus layers and the lateral particle spiral rings filling nuclear number increase, gradually saturated, nuclear power load distribution of the edge of the diffusion layer gradually thinning.

If a pair of particles spiral rings, high low π^{+}muon same direction of the wave motion, see figure 7.2; High and low π^{+}violation can only in the direction of the adjacent particles spiral wave motion transition in the ring. By the relationship of the space, the same layer, low-energy particle spiral rings π_g^{+}, π_d^{-} or π_g^{-}, π_d^{+} combination of lateral migration. Due to the symmetry, the first floor there are 12 seating arrangement, 2, 3, 4 layer respectively in 12, 6, 6 seating arrangement, a total of 36 seating arrangement. By figure 13.1 shows, between the upper and the lower migration, 1 ~ 2 layer particles spiral ring in five transitions. 2 ~ 3, 3 ~ 4 layer between respectively have four, three, a total of 12 channel. If each channel is π_g^{+},π_d^{-} or π_g^{-},π_d^{+} combination of transition, it also have 36 seating arrangement.

To the nucleus internal excess π^{+}violation of saturated layer, unable to increase; Adjust some of the seating arrangement will make mother nuclear total energy increases, it can only be achieved under the external energy to participate in; Most minor adjustment in the edge of the nucleus, will make the nuclear energy is reduced, to get through the formation of neutrino γ rays. Due to the different positions within the nucleus of the excess π^{+}muon distribution, lateral migration, the lower level migration, transition to another position, the electric and magnetic energy change value is not the same. The table 9.1 shows that transition between adjacent layers will lead to high, low π^{+}muon original the slight variations of wave energy. So, different size of nuclei formation energy spectrum of the γ rays, combination and different features, these can only through the calculation of concrete examples to illustrate.

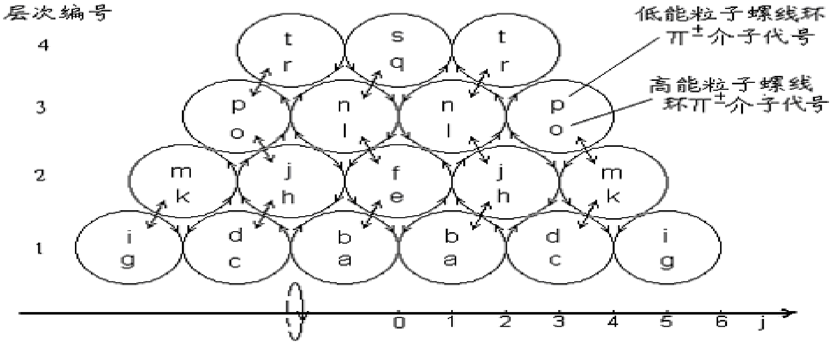

图13.1 原子核内净剩π±介子跃迁通道示意图

13.2 □Ray energy parameters calculation model

13.2.1 $^{194}_{79}$Au, $^{194}_{78}$Pt nucleus internal structure and parameter Calculation

$^{194}_{79}$Au nuclide atomic energy is 193.965406 u, 39.5 hours half-life, and magnetic $\pm 0.074 U_p$. Launch β^{+} rays, electron kinetic energy is 1.487, 1.230, 0.950 Mev three groups. Decay into $^{194}_{78}$Pt nucleus in the process of the communist party of China launch 49 level of γrays, energy distribution range of 0.20291 ~ 2.1142 Mev [4], eventually become a stable $^{194}_{78}$Pt nucleus. So, we could start from decay and the internal structure of two nuclei model, calculation and analysis to γrays forming principle and energy.

For $^{194}_{79}$Au nucleus, refer to section 12.1 for the magnetic moment of a nucleus simulation method. Make protons, neutrons according to figure 7.4 a, c, or b, d scheme "decentralized", from table 9.1, 7.4 (1) type, $^{194}_{79}$Au nucleus combined magnetic and can be expressed as:

$$\sum U = U^{+}_{g1} + U^{-}_{g1} + U^{+}_{g4} + 2U^{-}_{d1} + U^{+}_{d2} + U^{+}_{d3} = -0.07325U_{p} \qquad (13.1)$$

Take a and d state combination, by (7.4-2) type:

$$\sum U = 2U^{+}_{g1} + U^{+}_{g4} + U^{+}_{d1} + U^{-}_{d2} + U^{-}_{d3} + U^{-}_{d4} = 0.07325U_{p} \qquad (13.2)$$

If according to (13.2) type magnetic combination of calculation model, have $\pi^{\pm}$ both original energy increment: $\Delta\overline{m}$ =6.081173925×10 $^{-30}$Kg.

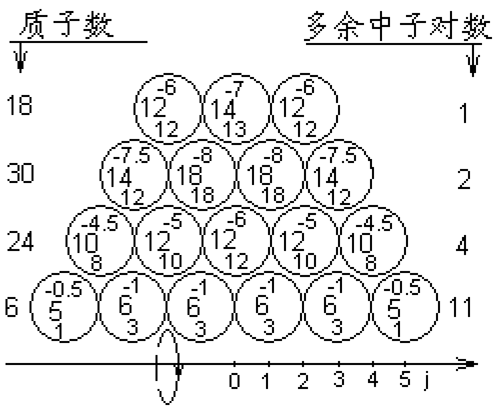

图 13.2 $^{194}_{79}Au$ 原子核内核子、净剩 $\pi^{\pm}$ 介子分配示意图

$V_a{}_{6}$ $\quad {}^{6}V_b{}_{-2}$ $\quad {}^{4}V_c{}_{6}$ $\quad {}^{10}V_d{}_{-2}$ $\quad {}^{8}V_e{}_{12}$ $\quad {}^{20}V_f{}_{-6}$

${}^{14}V_g{}_{2}$ $\quad {}^{16}V_h{}_{20}$ $\quad {}^{36}V_i{}_{-1}$ $\quad {}^{35}V_j{}_{-10}$ $\quad {}^{25}V_k{}_{16}$ $\quad {}^{41}V_l{}_{36}$

${}^{77}V_m{}_{-9}$ $\quad {}^{68}V_n{}_{-16}$ $\quad {}^{52}V_o{}_{24}$ $\quad {}^{76}V_p{}_{-15}$ $\quad {}^{61}V_q{}_{13}$ $\quad {}^{74}V_r{}_{24}$

${}^{98}V_s{}_{-7}$ $\quad {}^{91}V_t{}_{-12}$

$$W_{e} = 1.401321064\times10^{-27}Kg$$

$$W_{b} = 7.827518402\times10^{-30}Kg$$

$$\sum {}^{194}_{79}AuW_{1} = 3.220247476\times10^{-25}Kg$$

Refer to section 11.2 of the nucleus structure model, design and energy balance calculation procedures, the nuclear force numerical comparison results. The design of the $^{194}_{79}$Au, $^{194}_{78}$Pt nucleus internal structure is shown in figure 13.2 and figure 13.3; nuclear force balance test results see table 13.1 and table 13.2. $^{194}_{79}$ Au, $^{194}_{78}$Pt of the experimental value of nuclear energy, respectively:

$$\sum {}^{194}_{79}AuW_{0} = 3.220244434\times10^{-25}Kg$$

$$\sum {}^{194}_{78}PtW_{0} = 3.220208825\times10^{-25}Kg$$

$^{194}_{79}$Au nucleus nuclear force balance to verify the results table (figure 13.2, the unit: Newton) table 13.1

j / N_a	1	2	3	4	5	nuclearElectric and magnetic field force accumulated	
58 $F_{e\theta}$ $F_{b\theta}$		t. 597.2865265 -623.6670342				↑	-538.2026478
34 $F_{e\theta}$ $F_{b\theta}$	n. 845.3021482 -1222.642839		p. 891.0114236 -1146.227662			|	-511.8221401
16 $F_{e\theta}$ $F_{b\theta}$		j. 838.0225225 -786.4485285		m. 106.3890735 -598.8363964		|	-256.6059021
$F_{e\theta}$ 34/13 $F_{b\theta}$ $\Delta F_{\theta b}$	b. 256.935313 -14.26555772		d. 360.3313781 -14.26555772 -134.0624443		i. –2.039445479 -7.13277886 -57.45533327		388.0455737

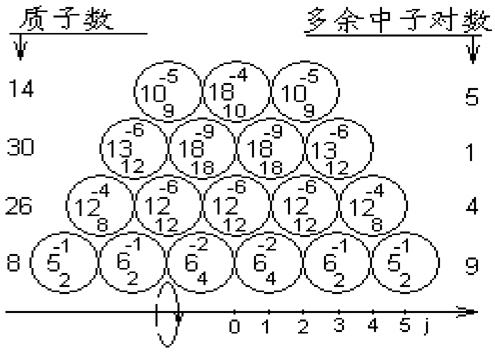

图 13.3 $^{194}_{78}Pt$ 原子核内核子、净剩 $\pi^{\pm}$ 介子分配示意图

$$Va_{8} \quad Vb^{8}_{-4} \quad Vc^{4}_{4} \quad Vd^{8}_{-2} \quad Ve^{6}_{12} \quad Vf^{18}_{-6}$$

$$Vg^{12}_{4} \quad Vh^{16}_{24} \quad Vi^{40}_{-2} \quad Vj^{38}_{-12} \quad Vk^{26}_{16} \quad Vl^{42}_{36}$$

$$Vm^{78}_{-8} \quad Vn^{70}_{-18} \quad Vo^{52}_{24} \quad Vp^{76}_{-12} \quad Vq^{64}_{10} \quad Vr^{74}_{18}$$

$$Vs^{92}_{-4} \quad Vt^{88}_{-10}$$

$$W_e = 1.392890861 \times 10^{-27} Kg$$

$$W_b = 9.474618808 \times 10^{-30} Kg$$

$$\sum {}^{194}_{79}PtW_1 = 3.220213937 \times 10^{-25} Kg$$

To mother nuclear $^{194}_{79}$Au, $^{194}_{78}$Pt internal structure comparison, can see mother son become nuclear fission failure when net with high and low $\pi^{\pm}$muon and extra neutron to adjust the migration trend. By the law of conservation of energy, we can calculate $^{194}_{79}$Au every position in nucleus, each net with high and low $\pi^{\pm}$ violation or to each pair of $\pi^{\pm}$violation adjustment migration when launching the γ ray energy. It must be pointed out that this is just our ideal model. By this model, we can see by the numerous nuclides $^{194}_{79}$Au→$^{194}_{78}$Pt, γrays in the process of energy spectrum, the trend of the chance.

$^{194}_{78}$Pt nucleus nuclear force balance test results see (figure 13.3, unit: N) table 13.2

j / N_a	1	2	3	4	5	nuclearElectric and magnetic field force accumulated	
58 $F_{e\theta}$ $F_{b\theta}$		t. 394.0283291 -296.984302				↑	-145.8833932

34 $F_{e\theta}$ $F_{b\theta}$	n. 799.4848898 -1547.407343	p. 1095.757365 -1031.604895		| |	-242.9274203
16 $F_{e\theta}$ $F_{b\theta}$		j. 1091.575393 -943.7382342	m. 76.90747548 -629.1588228	| |	-307.0798898
$F_{e\theta}$ 34/13 $F_{b\theta}$ $\Delta F_{\theta b}$	b. 352.2356112 -57.06223088 -137.8927999	d. 173.5481658 -28.53111544 -68.94639993	i. –52.80497456 -14.26555772 -68.94639993	| | |	97.33429869

13.2.2 γ ray spectrum simulation principle

The data in the table 9.1 shows that the net with high and low $\pi^{\pm}$mesons in different particles spiral ring transition between layer, due to the high and low $\pi^{\pm}$muon original wave motion direction of the original energy $\overline{m}_{gi}$, $\overline{m}_{di}$, a slight differences, so the total energy a little influence. Behind us in order to convenient calculation, first the energy difference between the value of $\Delta\overline{m}_{gi}$, $\Delta\overline{m}_{di}$, direct conversion into Mev, shown in table 13.3.

Each layer particles spiral rings are made by the original PI to wave energy is the same as $\pi^{\pm}$ violation, in addition to the net with $\pi^{\pm}$ violation of migration, antiparticle $\pi^{\pm}$ both migration is also exist. Position as shown in figure 13.1, p a low-energy π_d^- both migrated to m position, and can be expressed as $p\pi_d^- \rightarrow m\pi_d^-$. If antiparticle migration, the m position a low-energy π_d^+ muon migrated to p for nuclear power charge distribution adjustment effect is the same, only difference is calculated in table 13.3 nucleus total energy, $\Delta\overline{m}_{di}$ school when is take the positive or negative. It is in the law of conservation of energy, under the premise of judgment with net high and low $\pi^{\pm}$muon migration channel can be formed an important basis for adjustment.

Different particles spiral ring between $\pi^{\pm}$muon original energy

Differences $\Delta\overline{m}_{gi}$, $\Delta\overline{m}_{di}$, table 13.3

$N_{\alpha d,g}$ / $\overline{m}_{di.gi}$	$\frac{34}{13}$、$\frac{34}{13}$	16 50	34 114	58 203	88 316
$\overline{m}_{di}$, $\overline{m}_{gi}$ $\times 10^{-28} Kg$	3.304461327 6.608922653	3.348508963 6.550192473	3.325343178 6.581080185	3.316814573 6.592451659	3.312652281 6.598001381

$\Delta\overline{m}_{d(i\sim i+1)}$ $\times 10^{-30} Kg$ MeV		4.4047636 2.470890	2.3165785 1.299505	0.8528605 0.478419	0.4162292 0.233487	
$\Delta\overline{m}_{g(i\sim i+1)}$ $\times 10^{-30} Kg$ Mev		5.873018 3.294520	3.0887712 1.732673	1.1371474 0.637893	0.5549722 0.311316	

By know in chapter 11, 12, to split the decay naturally mother nucleus and the stability of the son, and there is a variety of meat with nuclear power. Laboratory detection to launch out 49 in the process of the decay of nuclear fission energy levels of γ rays is lucky and rock atomic number N_A constituting for coefficient of ${}^{194}_{79}$Au nuclei with nuclear power, in the process of decay released all the comprehensive results of γ ray spectrum. Most of the energy level of the γ rays appear less risk of poor, but also do not eliminate the energy behind the data error range is composed of several level is close to the results of the comprehensive reflection of γ rays. With existing experimental detection technology level, we can't separate detection to the whole process of the decay, with a particular internal structure, energy of ${}^{194}_{79}$Au nuclei with nuclear power, completely failure become stable another has certain internal structure, the level of ${}^{194}_{78}$Pt nuclei with nuclear power, in the whole process of all the γ ray energy spectrum and time sequence. In fact also doesn't exist the physical condition of the external environment. Because and thermodynamics of the statistical laws of gas molecules thermal motion completely, the entire field of neutrinos, one neutrino one at a time through the nucleus of a particular position, is completely random, unpredictable.

therefore, can think of: laboratory detected a γ ray energy levels and the risk of appear, is a large number of nuclei with nuclear power, ${}^{194}_{79}\mathrm{Au}\rightarrow{}^{194}_{78}\mathrm{Pt}$ during the whole process of split decay, a particular internal structure adjustment, specific energy of nuclide ${}^{194}_{79}$Au atoms, one of the characteristics of the location of the high and low $\pi^{\pm}$ muon migration, adjust to another level of nuclide ${}^{194}_{79}$Au atoms, or change to another ${}^{194}_{78}$Pt atoms nuclide characteristics of a certain position, excess energy release in the form of γ rays. Nuclide in gram atom coefficient as the unit of atoms, this process can only be the two ${}^{194}_{79}$Au, ${}^{194}_{78}$Pt atoms of two particular nuclides with nuclear power risk existing in the process of transformation, only statistical significance. We can't figure out, is the parent nucleus transformation before or after transformation launch γ rays.

So, we can use a kind of as shown in figure 13.2 ${}^{194}_{79}$Au the parent nucleus with nuclear power, as the reference standard. When its internal structure, nuclear and clean with $\pi^{\pm}$ mesons in total energy conservation under the premise of to the son, as shown in the figure 13.3 nuclear ${}^{194}_{78}$Pt with nuclear power, adjust the transformation, each γ ray energy that is released in the adjustment process, as the reference value of the γ ray energy spectrum. Obviously, it is only a small part of the actual γ ray spectrum of possible.

13.2.3 □ray energy spectrum of applications

According to the principle of γrays in the above form, design of γray spectrum calculation procedure is as follows:

1. According to section 11.2 nucleus total energy calculation procedure, we repeated computation as shown in the figure 13.2 ${}^{194}_{79}$Au nuclei with nuclear power of total energy $\sum{}^{194}_{79}\mathrm{Au}W_1=3.220247476\times10^{-25}\mathrm{Kg}$

2. According to the figure 13.1, high, low $\pi^{\pm}$muon possible migration channel, make $f\bar{\pi}\rightarrow b\bar{\pi}$, into another with nuclear power, 2, and the power, and nuclear energy calculation parameters of Vb ~ Vf of coefficient table 13.4 line 4; Other coefficient remain unchanged. Similarly, nucleus total magnetic energy will also change. Repeating section 11.2 1 ~ 12 calculation program: power, total energy 2 $\sum{}^{194}_{79}\mathrm{Au}W_2=3.220192308\times10^{-25}\mathrm{Kg}$

3. Make two states with nuclear power, the energy difference as ΔW_e:

$$\Delta W_e=\sum_{79}^{194}AuW_1-\sum_{79}^{194}AuW_2=3.094686Mev$$

For laboratory detects γ rays energy spectrum is the range of $0.20291_6 \sim 2.1142_2$ Mev, (subscript for terminal error range). $\Delta\overline{m}_{gi}$、 $\Delta\overline{m}_{di}$ Data from table 13.3, the total of the law of conservation of energy, is a particle transition, $f\pi^-\rightarrow b\pi^-$, the γray energy W_γ is:

$$W_\gamma=\sum_{79}^{194}AuW_1-\sum_{79}^{194}AuW_2+\Delta\overline{m}_{d(1\sim2)}=5.565576Mev;$$

Similarly, if the antiparticle transition, $b\pi^+\rightarrow f\pi^+$ to W_γ is:

$$W_\gamma=\sum_{79}^{194}AuW_1-\sum_{79}^{194}AuW_2-\Delta\overline{m}_{d(1\sim2)}=0.623796Mev;$$

The former far outweigh the laboratory value 2.1142 Mev, obviously does not exist, the latter is one of our expectations.

13.3 γ ray spectrum calculation example

To calculated according the above program, ${}_{79}^{194}Au\rightarrow{}_{78}^{194}Pt$ nucleus of γray spectrum simulation in table 13.4.

${}_{79}^{194}Au$ conditions within the nucleus on the lower $\pi^{\pm}$ muon warp gamma ray spectrum simulation table table 13.4

$\pi^{\pm}$Muon transition position	Electric energy coefficient changes	$\sum W_i\times10^{-25}$Kg $\sum W_0-\sum W_i$(Mev)	$\pi^{\pm}$ Muon transition way （W_γ=Mev）
$e\pi^+\rightarrow a\pi^+$	$\underset{7}{Va}\ \overset{7}{\underset{-2}{Vb}}\ \overset{5}{\underset{6}{Vc}}\ \overset{11}{\underset{-2}{Vd}}\ \overset{9}{\underset{11}{Ve}}$	3.220355938 -6.084245	
$e\pi^+\rightarrow a\pi^+$ $f\pi^-\rightarrow b\pi^-$	$\underset{7}{Va}\ \overset{7}{\underset{-3}{Vb}}\ \overset{4}{\underset{6}{Vc}}\ \overset{10}{\underset{-2}{Vd}}\ \overset{8}{\underset{11}{Ve}}\ \overset{19}{\underset{-5}{Vf}}$	3.220292476 -2.524305	
$f\pi^-\rightarrow b\pi^-$	$\overset{6}{\underset{-3}{Vb}}\ \overset{3}{\underset{6}{Vc}}\ \overset{9}{\underset{-2}{Vd}}\ \overset{7}{\underset{12}{Ve}}\ \overset{19}{\underset{-5}{Vf}}$	3.220192308 3.094736	$b\pi^+\rightarrow f\pi^+$ 0.623796
$h\pi^+\rightarrow a\pi^+$	$\underset{7}{Va}\ \overset{7}{\underset{-2}{Vb}}\ \overset{5}{\underset{6}{Vc}}\ \overset{11}{\underset{-2}{Vd}}\ \overset{9}{\underset{12}{Ve}}\ \overset{21}{\underset{-6}{Vf}}\ \overset{15}{\underset{2}{Vg}}\ \overset{17}{\underset{19}{Vh}}$	3.220371749 -6.971214	
$j\pi^-\rightarrow b\pi^-$ $h\pi^+\rightarrow a\pi^+$	$\underset{7}{Va}\ \overset{7}{\underset{-3}{Vb}}\ \overset{4}{\underset{6}{Vc}}\ \overset{10}{\underset{-2}{Vd}}\ \overset{8}{\underset{12}{Ve}}\ \overset{20}{\underset{-6}{Vf}}\ \overset{14}{\underset{2}{Vg}}\ \overset{16}{\underset{19}{Vh}}\ \overset{35}{\underset{-1}{Vi}}\ \overset{34}{\underset{-9}{Vj}}$	3.220290444 -2.410299	
$j\pi^-\rightarrow b\pi^-$	$\overset{6}{\underset{-3}{Vb}}\ \overset{3}{\underset{6}{Vc}}\ \overset{9}{\underset{-2}{Vd}}\ \overset{7}{\underset{12}{Ve}}\ \overset{19}{\underset{-6}{Vf}}\ \overset{13}{\underset{2}{Vg}}\ \overset{15}{\underset{20}{Vh}}\ \overset{35}{\underset{-1}{Vi}}\ \overset{34}{\underset{-9}{Vj}}$	3.220175306 4.048447	$b\pi^+\rightarrow j\pi^+$ 1.577557
$h\pi^+\rightarrow c\pi^+$	$\overset{4}{\underset{7}{Vc}}\ \overset{11}{\underset{-2}{Vd}}\ \overset{9}{\underset{12}{Ve}}\ \overset{21}{\underset{-6}{Vf}}\ \overset{15}{\underset{2}{Vg}}\ \overset{17}{\underset{19}{Vh}}$	3.220300167 -2.955736	$c\pi^-\rightarrow h\pi^-$ 0.338784
$j\pi^-\rightarrow d\pi^-$ $h\pi^+\rightarrow c\pi^+$	$\overset{4}{\underset{7}{Vc}}\ \overset{11}{\underset{-3}{Vd}}\ \overset{8}{\underset{12}{Ve}}\ \overset{20}{\underset{-6}{Vf}}\ \overset{14}{\underset{2}{Vg}}\ \overset{16}{\underset{19}{Vh}}\ \overset{35}{\underset{-1}{Vi}}\ \overset{34}{\underset{-9}{Vj}}$	3.220253522 -0.339149	$c\pi^-\rightarrow h\pi^-$ $d\pi^+\rightarrow j\pi^+$ 0.484481
$j\pi^-\rightarrow d\pi^-$	$\overset{10}{\underset{-3}{Vd}}\ \overset{7}{\underset{12}{Ve}}\ \overset{19}{\underset{-6}{Vf}}\ \overset{13}{\underset{2}{Vg}}\ \overset{15}{\underset{20}{Vh}}\ \overset{35}{\underset{-1}{Vi}}\ \overset{34}{\underset{-9}{Vj}}$	3.220203747 2.453013	
$k\pi^+\rightarrow c\pi^+$	$\overset{4}{\underset{7}{Vc}}\ \overset{11}{\underset{-2}{Vd}}\ \overset{9}{\underset{12}{Ve}}\ \overset{21}{\underset{-6}{Vf}}\ \overset{15}{\underset{2}{Vg}}\ \overset{17}{\underset{20}{Vh}}\ \overset{37}{\underset{-1}{Vi}}\ \overset{36}{\underset{-10}{Vj}}\ \overset{26}{\underset{15}{Vk}}$	3.220339459 -5.159881	

$k\pi^+ \rightarrow c\pi^+ . m\pi^-$ $\rightarrow d\pi^-$	$Vc^{4}_{7}\ Vd^{11}_{-3}\ Ve^{8}_{12}\ Vf^{20}_{-6}\ Vg^{14}_{2}\ Vh^{16}_{20}\ Vi^{36}_{-1}\ Vj^{35}_{-10}\ Vk^{25}_{15}$ $Vl^{40}_{36}\ Vm^{76}_{-8}$	3.220260705 -0.7420794	$d\pi^+ \rightarrow m\pi^+$. $c\pi^- \rightarrow k\pi^-$ 0.081551
$m\pi^- \rightarrow d\pi^-$	$Vd^{10}_{-3}\ Ve^{7}_{12}\ Vf^{19}_{-6}\ Vg^{13}_{2}\ Vh^{15}_{20}\ Vi^{35}_{-1}\ Vj^{34}_{-10}\ Vk^{24}_{16}\ Vl^{40}_{36}\ Vm^{76}_{-8}$	3.22017302 4.176686	$d\pi^+ \rightarrow m\pi^+$. 1.705796
$k\pi^+ \rightarrow g\pi^+$	$Vg^{14}_{3}\ Vh^{17}_{20}\ Vi^{37}_{-1}\ Vj^{36}_{-10}\ Vk^{26}_{15}$	3.220297748 -2.820064	$g\pi^- \rightarrow k\pi^-$ 0.474456
$k\pi^+ \rightarrow g\pi^+$ $m\pi^- \rightarrow i\pi^-$	$Vg^{14}_{3}\ Vh^{17}_{20}\ Vi^{37}_{-2}\ Vj^{35}_{-10}\ Vk^{25}_{15}\ Vl^{40}_{36}\ Vm^{76}_{-8}$	3.220259066 -0.650160	$i\pi^+ \rightarrow m\pi^+$. $g\pi^- \rightarrow k\pi^-$ 0.173470
$m\pi^- \rightarrow i\pi^-$	$Vi^{36}_{-2}\ Vj^{34}_{-10}\ Vk^{24}_{16}\ Vl^{40}_{36}\ Vm^{76}_{-8}$	3.22021208 2.090572	
$l\pi^+ \rightarrow e\pi^+$	$Ve^{8}_{13}\ Vf^{21}_{-6}\ Vg^{15}_{2}\ Vh^{17}_{20}\ Vi^{37}_{-1}\ Vj^{36}_{-10}\ Vk^{26}_{16}\ Vl^{42}_{35}$	3.220308713 -3.435152	
$l\pi^+ \rightarrow e\pi^+$ $n\pi^- \rightarrow f\pi^-$	$Ve^{8}_{13}\ Vf^{21}_{-7}\ Vg^{14}_{2}\ Vh^{16}_{20}\ Vi^{36}_{-1}\ Vj^{35}_{-10}\ Vk^{25}_{16}\ Vl^{41}_{35}\ Vm^{76}_{-9}\ Vn^{67}_{-15}$	3.220239193 0.464617	$f\pi^+ \rightarrow n\pi^+\ e\pi^- \rightarrow l\pi^-$ 0.031449 $l\pi^+ \rightarrow e\pi^+\ n\pi^- \rightarrow f\pi^-$ 0.897785
$n\pi^- \rightarrow f\pi^-$	$Vf^{20}_{-7}\ Vg^{13}_{2}\ Vh^{15}_{20}\ Vi^{35}_{-1}\ Vj^{34}_{-10}\ Vk^{24}_{16}\ Vl^{40}_{36}\ Vm^{76}_{-9}\ Vn^{67}_{-15}$	3.220179757 3.798768	$n\pi^- \rightarrow f\pi^-$ 2.499263
$l\pi^+ \rightarrow h\pi^+$	$Vh^{16}_{21}\ Vi^{37}_{-1}\ Vj^{36}_{-10}\ Vk^{26}_{16}\ Vl^{42}_{35}$	3.220292902 -2.548183	
$l\pi^+ \rightarrow h\pi^+$ $n\pi^- \rightarrow j\pi^-$	$Vh^{16}_{21}\ Vi^{37}_{-1}\ Vj^{36}_{-11}\ Vk^{25}_{16}\ Vl^{41}_{35}\ Vm^{76}_{-9}\ Vn^{67}_{-15}$	3.220241025 0.361859	$l\pi^+ \rightarrow h\pi^+\ n\pi^- \rightarrow j\pi^-$ 0.795027
$n\pi^- \rightarrow j\pi^-$	$Vj^{35}_{-11}\ Vk^{24}_{16}\ Vl^{40}_{36}\ Vm^{76}_{-9}\ Vn^{67}_{-15}$	3.220196759 2.845007	$n\pi^- \rightarrow j\pi^-$ 1.545502
$o\pi^+ \rightarrow h\pi^+$	$Vh^{16}_{21}\ Vi^{37}_{-1}\ Vj^{36}_{-10}\ Vk^{26}_{16}\ Vl^{42}_{36}\ Vm^{78}_{-9}\ Vn^{69}_{-16}\ Vo^{53}_{23}$	3.220323499 -4.264582	
$o\pi^+ \rightarrow h\pi^+$ $p\pi^- \rightarrow j\pi^-$	$Vh^{16}_{21}\ Vi^{37}_{-1}\ Vj^{36}_{-11}\ Vk^{25}_{16}\ Vl^{41}_{36}\ Vm^{77}_{-9}\ Vn^{68}_{-16}\ Vo^{52}_{23}\ Vp^{75}_{-14}$	3.220245594 0.105570	$o\pi^+ \rightarrow h\pi^+\ p\pi^- \rightarrow j\pi^-$ 0.538738
$p\pi^- \rightarrow j\pi^-$	$Vj^{35}_{-11}\ Vk^{24}_{16}\ Vl^{40}_{36}\ Vm^{76}_{-9}\ Vn^{67}_{-16}\ Vo^{51}_{24}\ Vp^{75}_{-14}$	3.220171221 4.277613	
$o\pi^+ \rightarrow k\pi^+$	$Vk^{25}_{17}\ Vl^{42}_{36}\ Vm^{78}_{-9}\ Vn^{69}_{-16}\ Vo^{53}_{23}$	3.220284207 -2.060437	
$o\pi^+ \rightarrow k\pi^+$ $p\pi^- \rightarrow m\pi^-$	$Vk^{25}_{17}\ Vl^{42}_{36}\ Vm^{78}_{-10}\ Vn^{68}_{-16}\ Vo^{52}_{23}\ Vp^{75}_{-14}$	3.220238175 0.521720	$m\pi^+ \rightarrow p\pi^+\ k\pi^- \rightarrow o\pi^-$ 0.088522 $o\pi^+ \rightarrow k\pi^+\ p\pi^- \rightarrow m\pi^-$ 0.954888
$p\pi^- \rightarrow m\pi^-$	$Vm^{77}_{-10}\ Vn^{67}_{-16}\ Vo^{51}_{24}\ Vp^{75}_{-14}$	3.220201948 2.553941	$p\pi^- \rightarrow m\pi^-$ 1.254436
$q\pi^+ \rightarrow l\pi^+$	$Vl^{41}_{37}\ Vm^{78}_{-9}\ Vn^{69}_{-16}\ Vo^{53}_{24}\ Vp^{77}_{-15}\ Vq^{62}_{12}$	3.220315827 -3.834195	
$q\pi^+ \rightarrow l\pi^+$ $s\pi^- \rightarrow n\pi^-$	$Vl^{41}_{37}\ Vm^{78}_{-9}\ Vn^{69}_{-17}\ Vo^{52}_{24}\ Vp^{76}_{-15}\ Vq^{61}_{12}\ Vr^{73}_{24}\ Vs^{97}_{-6}$	3.220252627 -0.288933	$q\pi^+ \rightarrow l\pi^+$ $n\pi^+ \rightarrow s\pi^+$ 0.827379

$s\pi^- \rightarrow n\pi^-$	$Vn^{68}_{-17}\ Vo^{51}_{24}\ Vp^{75}_{-15}\ Vq^{60}_{13}\ Vr^{73}_{24}\ Vs^{97}_{-6}$	3.220185034 3.502738	
$r\pi^+ \rightarrow l\pi^+$ $t\pi^- \rightarrow n\pi^-$	$Vl^{41}_{37}\ Vm^{78}_{-9}\ Vn^{69}_{-17}\ Vo^{52}_{24}\ Vp^{76}_{-15}\ Vq^{61}_{13}\ Vr^{74}_{23}\ Vs^{97}_{-7}\ Vt^{90}_{-11}$	3.220252345 -0.273141	$r\pi^+ \rightarrow l\pi^+$ $n\pi^+ \rightarrow t\pi^+$ 0.843171
$t\pi^- \rightarrow n\pi^-$	$Vn^{68}_{-17}\ Vo^{51}_{24}\ Vp^{75}_{-15}\ Vq^{60}_{13}\ Vr^{73}_{24}\ Vs^{97}_{-7}\ Vt^{90}_{-11}$	3.220175644 4.029504	
$r\pi^+ \rightarrow o\pi^+$	$Vo^{52}_{25}\ Vp^{77}_{-15}\ Vq^{62}_{13}\ Vr^{75}_{23}$	3.220294461 -2.635665	
$r\pi^+ \rightarrow o\pi^+$ $t\pi^- \rightarrow p\pi^-$	$Vo^{52}_{25}\ Vp^{77}_{-16}\ Vq^{61}_{13}\ Vr^{74}_{23}\ Vs^{97}_{-7}\ Vt^{90}_{-11}$	3.220247685 -0.011747	$r\pi^+ \rightarrow o\pi^+$ $t\pi^- \rightarrow p\pi^-$ 0.147727 $r\pi^+ \rightarrow o\pi^+$ $p\pi^+ \rightarrow t\pi^+$ 1.104565
$t\pi^- \rightarrow p\pi^-$	$Vp^{76}_{-16}\ Vq^{60}_{13}\ Vr^{73}_{24}\ Vs^{97}_{-7}\ Vt^{90}_{-11}$	3.220201183 2.596849	$t\pi^- \rightarrow p\pi^-$ 2.118430
note	W_γ field, part of the γ ray energy spectrum calculation result is negative, the part beyond the experimental range, are no longer to calculate.		